A Prosthetic Ankle Design to Improve Stair Ambulation for Transfemoral Amputees

David Jonsson

A Thesis

Submitted in partial fulfillment of the

Requirements for the degree of

Master of Science in Mechanical Engineering

University of Washington

2015

Committee

Brian C. Fabien, Chair

Katherine M. Steele

Duane Storti

Program Authorized to Offer Degree:

Department of Mechanical Engineering

University of Washington

Abstract

A Prosthetic Ankle Design to Improve Stair Ambulation for Transfemoral Amputees

David Jonsson

Chair of the Supervisory Committee:
Professor Brian C. Fabien
Department of Mechanical Engineering

The aim of this thesis is to design a prosthetic ankle to improve stair ambulation for transfemoral (above knee) amputees.

Even though many prosthetic knees offer stair descent capabilities, no prosthetic ankle provides a natural stair descent gait for transfemoral amputees. Most ankles have a limited range of motion resulting in transfemoral amputees placing their heel on the edge of the step and rolling over the foot. This causes increased loads on the intact limb as well as increased risk of falling.

This thesis presents a prosthetic ankle design that provides the user with a more natural stair descent gait by allowing the ankle to move into dorsiflexion (toe points up) during stair descent.

As a part of the design process a gait analysis study is conducted. Transfemoral amputee stair descent gait is recorded and the results presented. The final design is presented along with a finite element analysis.

The presented design will help reduce the increased loads acting on the intact limb and likely reduce the risk of knee pain developing in transfemoral amputees' intact leg. It will also reduce the risk of falling by allowing a greater amount of the foot to remain in the step during stair descent.

Table of Contents

List of Figures

List of Tables

Acknowledgements

I would like to thank those that helped me on the journey that this Master‘s project has been. First and foremost I would like to thank Professor Brian Fabien for his constant guidance and great advice which made this project possible. I would also like to thank Professor Katherine Steele for her help on the biomechanics aspect of my project. To my fellow graduate students I would like to say thank you, especially my friend Tony Enslow who suffered through multiple revisions of my work. Last but certainly not least I would like to thank my wife for her endless support and faith in me during this project. Without their help this would not have been possible.

1 Introduction and background

1.1 Introduction

Ambulating stairs is a task most people spend little time thinking about, let alone worry about. For amputees this is another story. Stairs can be a source of anxiety and are often avoided to prevent accidents or injuries. Most modern day prosthetics aim to improve walking gait but often fall short when it comes to less frequent movements like stairs, small steps, and turning.

With technology growing exponentially one could have expected prosthetic feet to have advanced further than the biological one. This is unfortunately not the case and even such trivial things as descending stairs has yet to be mastered by a prosthetic foot. During stair descent the ankles range of motion is ~60-70°, starting out in ~25-30° of plantarflexion (toe points down) and moving into 35-40° of dorsiflexion (toe points up) during stance [1, 33]. Most prosthetic ankles are stiff, made from carbon fiber or similar materials, and provide little movement during stair descent. There are a few ankles designed with slightly greater range of motion but none that successfully mimics the natural stair descent of able-bodied individuals.

This thesis presents a novel prosthetic ankle design for improved stair ambulation. The designed ankle provides a greater range of motion during stair descent for a more natural gait. The aim of this thesis is to thoroughly cover the design process of a prosthetic ankle. During the design process a gait analysis study was performed on transfemoral (above knee) amputee stair descent gait. The results of that study are presented as a vital part of the design criteria. To fully understand the need for the ankle presented in this thesis, it is important to provide a thorough explanation of the problem that amputees face when descending stairs.

1.2 Problem statement – Stair descent issues

Most people don‘t think too much about how they perform day-to-day activities. Standing up from a chair for example is not difficult but for someone who has had his leg amputated, the activity becomes more difficult. All balance moves over to the intact limb and many amputees stand up using just one leg. Standing up from a chair is not the only activity that causes a problem. Walking down stairs is another activity that can be challenging. Stair descent requires good control of the ankle, knee, and hip joints. For transtibial (below knee) amputees, stair descent is not too difficult as they still have two out of these three joints. For transfemoral (above knee) amputees, on the other hand, stair descent is quite a daunting task as they only have control of their hip joint and have to put their trust in the prosthetic components they are using. Figure 1.1 depicts the three joints during stair descent from stance phase to toe-off[1] for an able-bodied individual. In order to fully understand the problem amputees have with stair descent it is vital to understand how an able-bodied individual descends stairs.

[1] “The instant when the toe off the foot or shoe leaves the ground. Usually defines the end of stance and the start of swing.“[30]

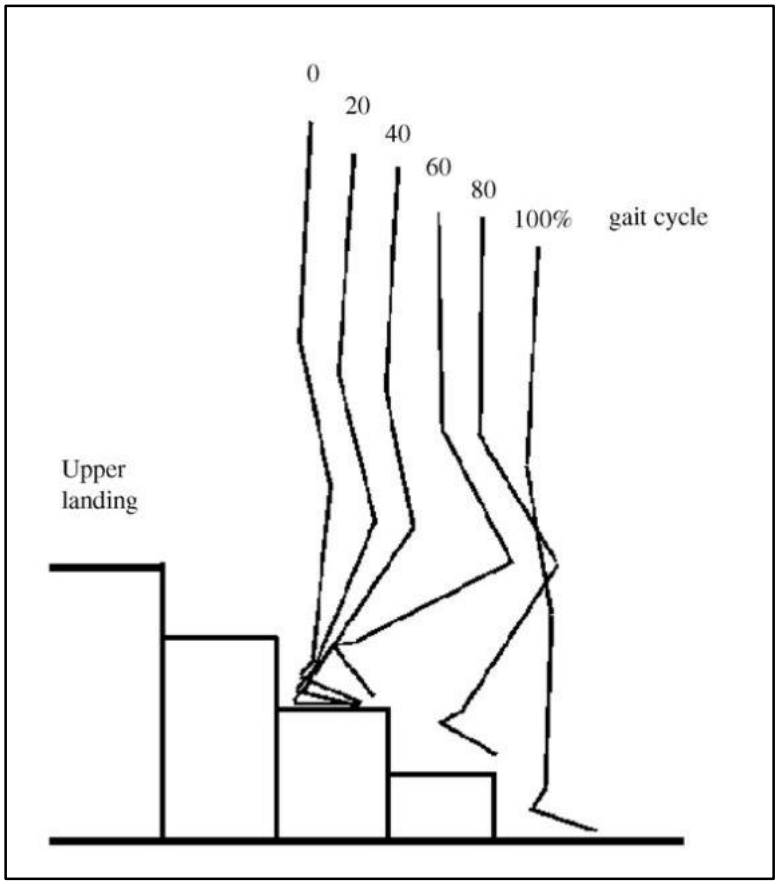

Figure 1.1: Normal stair descent gait for a single leg. Taken from [13]

We see from Figure 1.1 that at the beginning of stance phase the knee is slightly flexed, foot is plantarflexed (toe is down), and hip is also slightly flexed. During stance phase (0-40%), as the body moves over the foot the hip flexion stays similar but extends slightly towards the end of stance phase. Knee flexion gradually increases but the biggest change during stance phase occurs at the ankle. The ankle starts out in plantarflexion, at 0%, and then moves into dorsiflexion (toe is up), and reaches a maximum dorsiflexion just before toe off, at 60%. At toe off, the ankle joint gives a little push (plantarflexion) and the knee joint keeps flexing to prevent toe-drag when moving the leg into the next step (60%-100%). The hip joint flexes to move the thigh forward towards the next step. The ankle joint then moves into plantarflexion while the knee and hip joints extend to prepare for the next step.

By observing the aforementioned three joints, we can see where the challenges lie for transfemoral amputees. The hip joint, their remaining joint, has the smallest range of motion, during stance phase, while the knee and ankle joints need greater control and movement during normal stair descent. This affects transfemoral amputee stair descent gait. Several prosthetic knees are designed for stair descent gait by decelerating the knee joints angular velocity. Ankle solutions are not as effective for transfemoral amputees and most choose fixed angle dynamic elastic response prosthetic feet that store and return energy for damping and toe push-off [15].

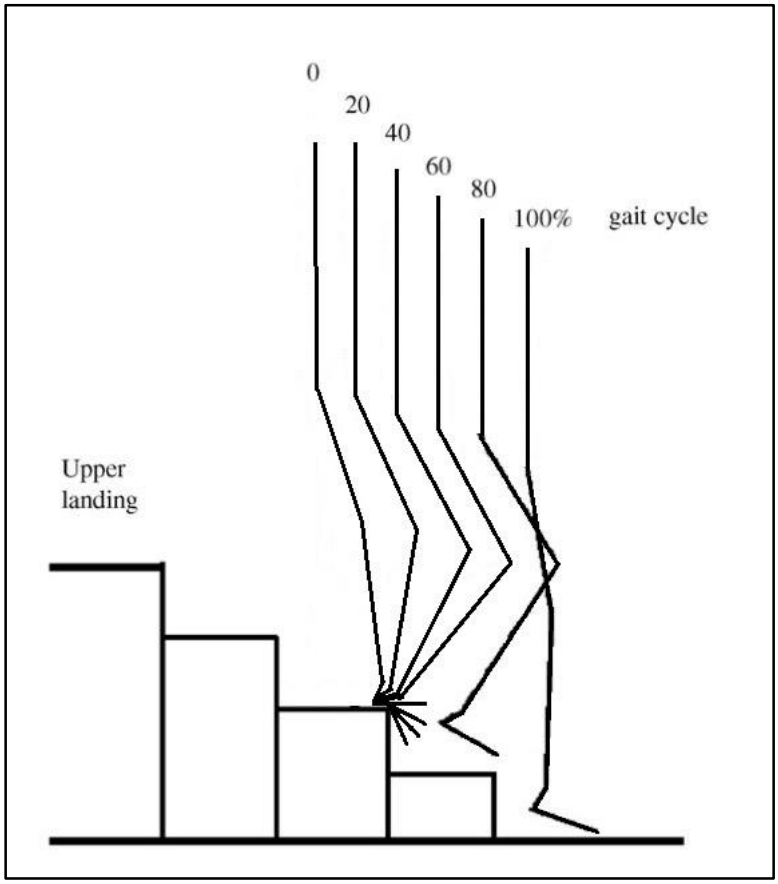

Figure 1.2: Normal prosthetic stair descent for a transfemoral amputee

Figure 1.2 depicts a transfemoral stair descent gait. Due to the limited ankle motion of the prosthetic foot they are often compared to walking in ski boots. Therefore transfemoral amputees "roll" the foot over the edge of the step [16]. T. Scmals et al showed that at 80% of stance phase

the prosthetic knee flexion increases rapidly and by the end of the stance phase it is greater than that of healthy individuals. They also showed a significant increase in the amount of peak flexion moment that affects the contralateral knee joint. Increased peaks of vertical and horizontal forces on the contralateral side indicate that the amputees "fall" onto the intact leg [16]. Transfemoral amputees are more than twice as likely to develop knee pain in the intact leg. Increased loads or gait abnormalities may cause this [17]. It is therefore important to develop prosthetic feet that mimic the natural stair descent gait better to preserve the intact knee joint.

Risk of falling is also increased during stair descent gait. Figure 1.3 shows the vertical ground reaction forces when descending one step.

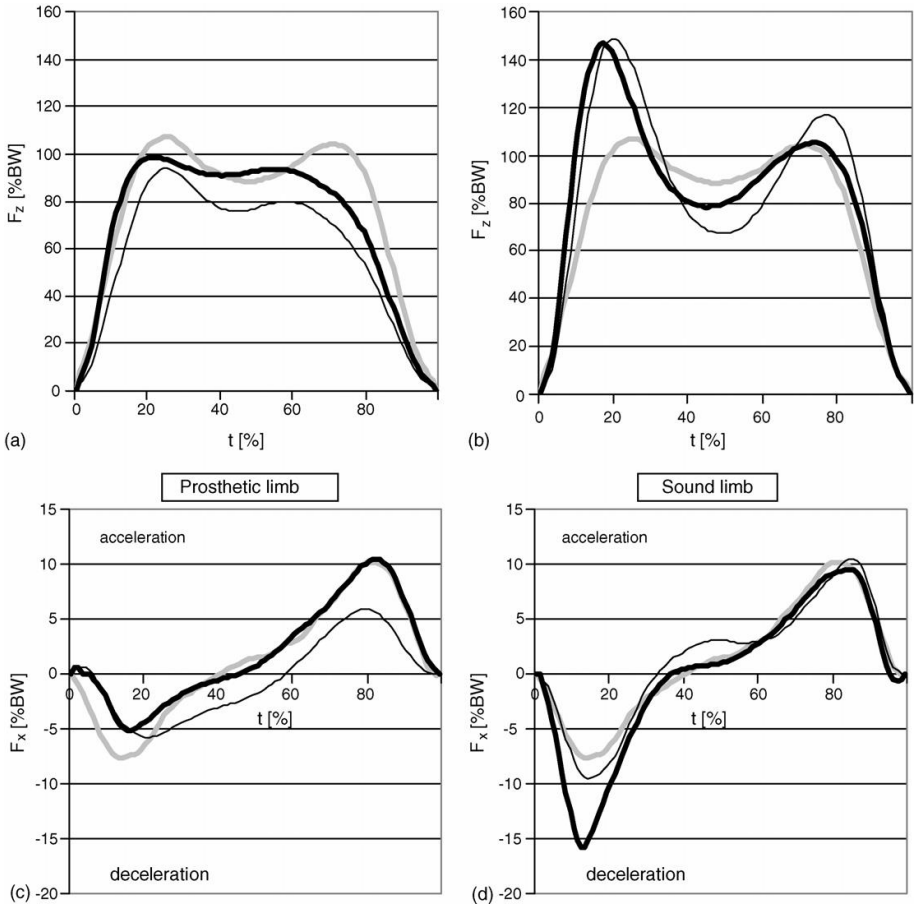

Figure 1.3: Ground reaction forces when descending one step. Figure taken from [16]. Thick black line shows transtibial amputees, thin black line shows transfemoral amputees, and the grey line shows the able-bodied.

The top two images of Figure 1.3 show the vertical ground reaction forces and the bottom two show the horizontal ground reaction forces acting forward. We see an increase in the vertical ground reaction force on the transfemoral amputees' intact limb at heel strike which corresponds to the increased loads discussed above. We also see a considerable decrease in the peak vertical ground reaction force for transfemoral amputees' prosthetic side. When comparing them to the able-bodied grey line, the first bump goes from ~110% for able-bodied to ~90-95% for transfemoral amputees but the second bump goes from ~110% to ~80%. If we now look at equation 1.1 for static friction

$$F_f = \mu * F_n \tag{1.1}$$

We see that the friction force F_f is equal to the coefficient of friction μ times the force normal to the surface F_n which in this case is the vertical ground reaction force. A reduction of the ground reaction forces coupled with a slippery surface will increase the risk of falling for a transfemoral amputee considerably as the amputee will slip as soon as the horizontal ground reaction force is greater than the friction force.

A prosthetic ankle design that would allow for natural stair descent gait could improve gait symmetry during stair descent, lower the impact forces and increased load on the intact limb, and reduce the risk of falling by increasing the ground reaction forces. The ankle would need to have a similar build height as other popular ankles on the market as well as being cheaper than or as expensive as ankles that offer similar properties. Such a design could benefit transfemoral amputees greatly and improve their quality of life. Chapter 2 describes a new ankle design for improved transfemoral amputee stair ambulation. It also discusses a stair descent study conducted to better understand transfemoral amputee gait.

1.3 Available prosthetic solutions

There are numerous knee solution currently available. Both active (motor-powered) and passive (not motor-powered) that are designed to assist transfemoral amputees descend stairs. These knees all work to decelerate the amputee during stair descent. These knees fall into three groups; hydraulic, magnetorheological, and motor powered, each group will be briefly described. Knee designs may differ slightly within a group but the main function remains the same.

Hydraulic knees use a hydraulic actuator to decelerate the knee joint. These knees generate great amounts of torque by controlling the flow of hydraulic fluid inside the actuator. When the knee joint moves, a piston is pushed down into a hydraulic cylinder. This motion forces hydraulic fluid to flow through a valve into another chamber. The breaking force is generated by controlling the opening of the valve. Figure 1.2 shows one of the most popular hydraulic knees, the C-leg by Otto Bock Inc. [32].

Figure 1.4: Image on left: The C-leg, taken from: http://www.koppers.nu/cleg.html
Image on right: stair descent using the C-leg, taken from: http://www.horizonprolabs.com/products.htm

There are also some hydraulic knees based on rotary hydraulics but they are not as common and will therefore be excluded.

Magnetorheological knees use magnetorheological fluid and a magnetic field to generate friction forces. When a magnetorheological fluid is subject to a magnetic field the metal particles in the fluid line up. By putting this fluid in between a moving object and a stationary one it is possible to generate breaking forces by lining the metal particles up between the two objects to generate friction between them. Figure 1.3 shows the magnetorheologically controlled Rheo knee by Ossur Inc. A more thorough description of the Rheo knee is given in chapter 2.

Figure 1.5: Rheo knee.
Image taken from: http://www.ossur.co.uk/rheoknee/

Motor powered knees are the last group. These knees use a motor to compensate for amputees' lost muscle power. By using a motor the knee can move independently of the user's leg and both power the user up from a chair or a flight of stairs as well as flexing the knee to increase ground clearance. They can also use motor power to extend the knee in strong headwinds, high grass, or snow. During stairs descent they do however work similar to the passive knees by decelerating the

knee joint. Figure 1.4 shows the Power knee by Ossur Inc. Power knee is currently the only motor-powered prosthetic knee commercially available but others are being developed at universities [14].

Figure 1.6: The Power knee.
Image taken from: http://www.ossur.com/prosthetic-solutions/bionic-technology/power-knee

Even though there are three groups of stair descending knee prostheses, all of them descend stairs in a similar way. By means of breaking the knee joint, reducing angular velocity, and allowing the user to walk step-over-step downstairs. These knees do not provide the user with much control of the stair descent gait, aside from the angular velocity, and transfemoral stair descent gait has thus often been described as controlled falling from one step to the next.

The variety of ankles with stairs descent features is not as great as the knees. There are a few prosthetic ankles that allow for plantarflexion and dorsiflexion, and even some with built in stairs descent features, but none that are specifically designed for transfemoral amputee stair descent gait. Figure 1.5 shows commercially available prosthetic ankle/feet that have

dorsiflexion/plantarflexion capabilities. A brief explanation of each device follows including stair descent properties.

Figure 1.7: a) Motionfoot MX by Fillauer, image taken from: http://www.ortoped.ca/en/motion-foot-sup-tm-sup-mx.html
b) Kinterra by Freedom-Innovations, image taken from: http://www.freedom-innovations.com/kinterra/
c) The Powerfoot Biom ankle, image taken from: https://www.soldiersocks.org/?page_id=7914
d) Proprio foot by Ossur, image taken from: http://www.ossur.com/prosthetic-solutions/bionic-technology/proprio-foot
e) Odyssey ankle by SpringActive, image taken from: http://www.springactive.com/odyssey.php
f) élan ankle by Endolite, image taken from: http://www.endolite.com/products/elan

Motionfoot MX is a rotary hydraulic foot developed by Fillauer. It has no electronics control but flexion damping is controlled using screws on the front. Like the other feet in Figure 1.6 it has a carbon fiber foot plate for improved walking gait and energy return to help with toe-off. It provides a 50° range of motion but most of that movement is plantarflexion. It does allow for up to 10° dorsiflexion by loosening the side plate and moving the pyramid, but due to the shape and location of the housing, dorsiflexion is limited to 10°. The foot makes stair descent more problematic for transfemoral amputees, as the ankle requires the ball of the foot to be on the step to prevent plantarflexion. Transfemoral amputee gait keeps the ball of the foot over the edge of the step,

which forces the ankle into plantarflexion and increases the risk of catching the toe on the next step. There is a manual lock on the ankle which prevents any movement, but engaging the lock before every staircase is tedious, for the user. [18]

Kinterra foot by Freedom-innovations is a hydraulic foot and uses a hydraulic cylinder to allow dorsi-/plantarflexion. It has a 12° range of motion, 10° plantarflexion and 2° dorsiflexion. It is designed to stay in dorsiflexion during swing phase in level ground walking to provide greater toe-clearance. It has no electronic control and hydraulic resistance is controlled using a screw on the side. Due to the limited range of motion in dorsiflexion it would not benefit transfemoral amputees in stairs descent but might improve stability on uneven terrain and slopes. [19]

The Biom foot is a motor-powered foot originally developed at the Massachusetts Institute of Technology (MIT). The ankle has a carbon fiber foot plate. It has a 200W brushless DC motor and a ball screw transmission. The actuator is in series with a carbon-fiber leaf spring and in parallel with a unidirectional leaf spring. The ankle is 2kg and provides a peak torque of 125Nm. It has been shown to have similar walking dynamics as the human ankle and has also been shown to improve amputee metabolic energy considerably [20, 21]. The ankle has a stair descent function to improve stair descent gait. The stair descent function is designed for transtibial amputees but does not improve transfemoral amputee stair descent gait much. The ankle goes into plantarflexion during swing to prepare for the next step. Then during stance it dorsiflexes until it reaches ~0° and stays at that angle until toe-off when it plantarflexes slightly to give a slight push forward [22]. The plantarflexion will not benefit transfemoral amputees; therefore, the Biom ankle provides a stair descent gait similar to a fixed ankle prosthesis.

The proprio foot is a motor-powered prosthetic ankle designed to improve walking on slopes, stairs, and level-ground. It has a DC step-motor that moves the carbon-fiber footplate when

unloaded [1]. It has 28° range of motion, 18° plantarflexion and 10° dorsiflexion [23]. It does have a stair descent function which only helps transtibial amputees. The ankle can only move the motor when unloaded, dorsiflexion is impossible during stance. Therefore the ankle dorsiflexes before stance and when transfemoral amputees land on a dorsiflexed foot it generates a flexion moment around the knee which does not improve stability, and often decreases it.

The Odyssey foot is the newest member to the bionic ankles and also has the least amount of documentation so the range of motion is not known. It uses a motor-spring to provide a powered walking gait. It has a user-specific spring in parallel with a small motor to provide a natural gait [24]. The ankle design is based on a prosthetic design, Sparky, from Arizona State University and was designed for transtibial amputees [25]. The author had the privilege of testing this ankle personally during an internship at Ossur Inc. in 2014 and can testify that it has the ability to move during stance. It also has a greater dorsiflexion than the Biom ankle but due to limited availability and published articles, stair descent gait for transfemorals is unknown.

The last ankle is the **élan** ankle. It has a carbon-fiber foot plate and a hydraulic cylinder that provides all movement. It is electronically controlled and weighs 1.2kg. It provides dorsi-/plantarflexion for improved walking on slopes and increased toe clearance during level-ground walking. It also increases stiffness in the hydraulics according to the terrain to improve gait by varying the movement and stiffness of the carbon foot plate [27]. Unfortunately, for transfemoral amputees, it provides the user with only 6° of plantarflexion and 3° of dorsiflexion [26] which is not enough to improve transfemoral stair descent gait.

2 The design process

The design process is split into three sections, each of which took approximately one quarter to finish. The first stage of the design process was to come up with three possible designs that could solve the problem at hand. These three design ideas will be described thoroughly along with the reasons why they could or could not work for this Master´s project. Following the design ideas are rough sketches of the proposed designs.

The second phase of the design process was to conduct a gait analysis study using human subjects. This was done to get realistic data of stair ambulation and especially stair descent. As this thesis had no funding and limited time, the analysis was limited to only two transfemoral amputees and one able bodied individual. Research description is clear enough to repeat the trial and gain further insight as well as to compare the data gained from this project to future studies.

The final design phase is the mechanical design itself. This involves the actual design process, conducted using Solidworks. Machining the ankle was beyond the scope of this project but all necessary drawings are included in this thesis to machine the item without any special knowledge from the author.

A fourth quarter was spent on the write-up and on further data processing, using Matlab, in order to present clear results. Some finite element analysis was also completed during the fourth quarter. A prototype was also 3D printed in order to give a physical understanding of the workings of the design. All these phases will be clearly described using figures, tables, and equations where appropriate.

2.1 Possible design 1

The first possible design idea is hydraulics based like the other two ideas. The benefits of a hydraulics system for this type of a prosthetic ankle is the great resistive force, low power consumption, and small size. It also provides the ability of movement during loading that most motors do not. Figure 2.1 shows a rough sketch of the ankle design.

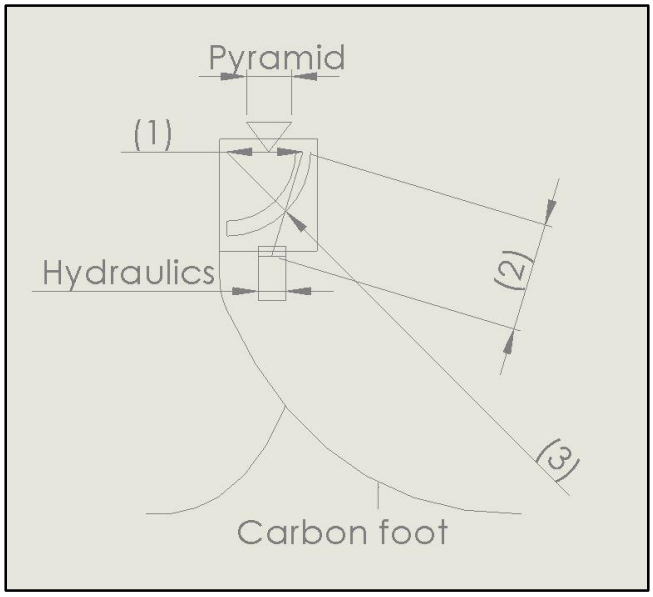

Figure 2.1: Design idea 1

The ankle depicted in Figure 2.1 would be fitted on the Vari-Flex with Evo made by Ossur Inc [8]. The pyramid would be a standard size prosthetic pyramid. (1) is a plate attached to the pyramid that is mounted on a hinge at the left end and connected to a rod at the right end. The rod (2) is fixed to a hydraulic cylinder and when the plate (1) moves down, following the circular path, the rod (2) pushes down on a hydraulic piston and the hydraulic cylinder (dashpot) will resist the motion. An electromechanical lock will hold the plate (1) in place, positioned at the connection of (1) and (2). This design will also need an inertial system to detect gait in order to properly control the opening and closing of the ankle system.

There are a few reasons why this design idea was not chosen for this project. Since this project needs to be manufacturable at the UW ME machine shop, the precision, tolerances, and size of the hydraulic cylinder will make it complicated to manufacture. If made bigger for simplicity, it would risk limiting the motion of the Vari-Flex foot plate. Another problem with this design is the requirement for two powered pieces, both the electromagnetic lock and a motor for the hydraulics to control fluid flow for variable resistance. Finally, this system might be difficult to make small enough without using expensive materials, and if made too big the loading point through the foot plate will be offset causing decreased benefits from the carbon foot.

2.2 Possible design 2

The second design idea is bigger and bulkier than design idea 1. Figure 2.2 shows a sketch of the basic function.

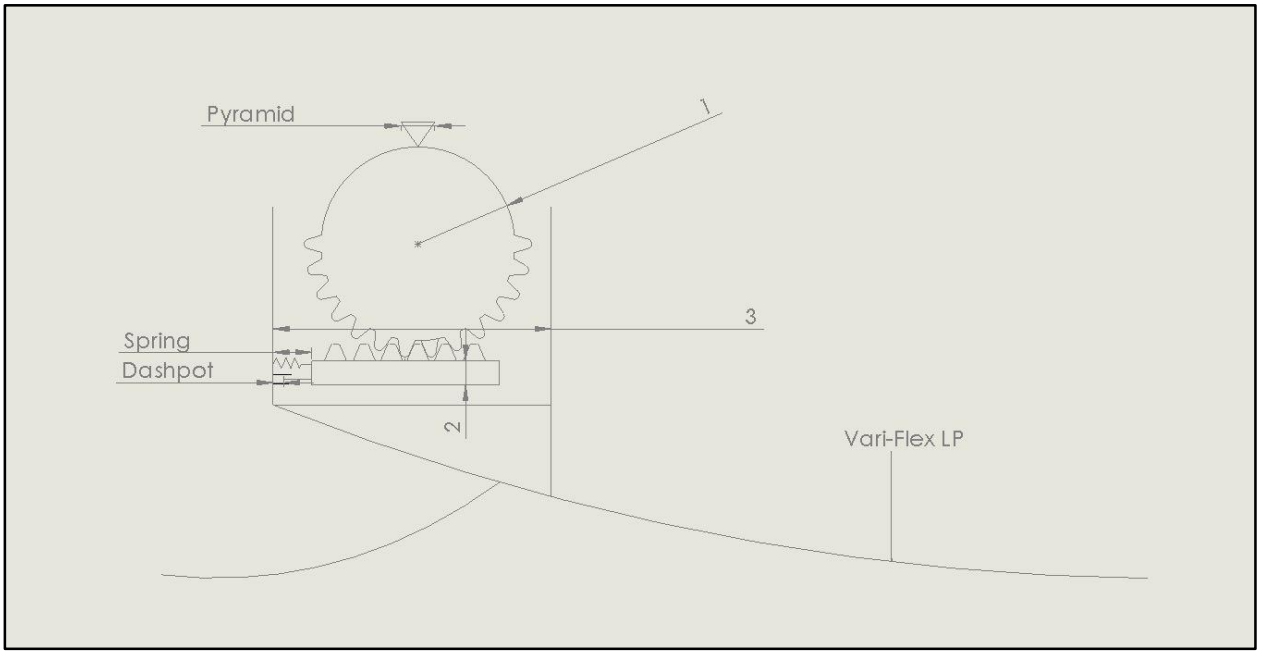

Figure 2.2: Design Idea 2

The ankle depicted in Figure 2.2 would be mounted on a LP Vari-Flex [9] which provides a smaller build height but a limited range of motion compared to the standard Vari-Flex foot plate used in

design idea 1. The pyramid is mounted on top of a cylinder (1) with a smooth top half, and a gear shape on the bottom half. The gears on the bottom half of (1) connect to gears on a sliding plate (2) that is fixed in place and allowed to move freely horizontally. The sliding plate (2) is connected to a spring and a dashpot which symbolize the hydraulic jack that would be connected there in a final design. When the pyramid is pointing straight up, as is shown in Figure 2.2, the spring will be fully extended. When the prosthetic user walks down stairs the dashpot provides resistance to control the rotational velocity of the cylinder (1). The resistance is controlled using a motor which operates a valve and controls the hydraulic flow inside the hydraulic jack. Movement is measured using inertial sensors i.e. accelerometers, gyroscopes, and magnetometers. Finally there is a box encompassing all the moving parts (3) that attaches to the carbon foot plate.

This design reduces the number of powered items from two, in design idea 1, to one. Overall size is also not as critical as in the previous design as it will not reduce any movement from the footplate. This design still has some great challenges. We are still using a hydraulic cylinder which increases tolerance requirements and reduces machinability, for the UW ME machine shop. Furthermore, due to heavy reliance on relatively small mechanical linkages, there are possible wear and tear issues with the gear and the sliding mechanism for the sliding plate. The gears will also require tight tolerances as any play in the gears will result in unwanted movement for the prosthetic user. The gears will also take up most of the force required to restrict all movement during level ground walking which will require stronger material for the gears and might cause some fatigue problems. Due to these challenges, this design was not chosen for this project.

2.3 Possible design 3

The third and final design idea was chosen as the final design for this project. Figure 2.3 shows a basic sketch of the main function of this design idea. Later in this chapter a thorough design will be presented for this idea.

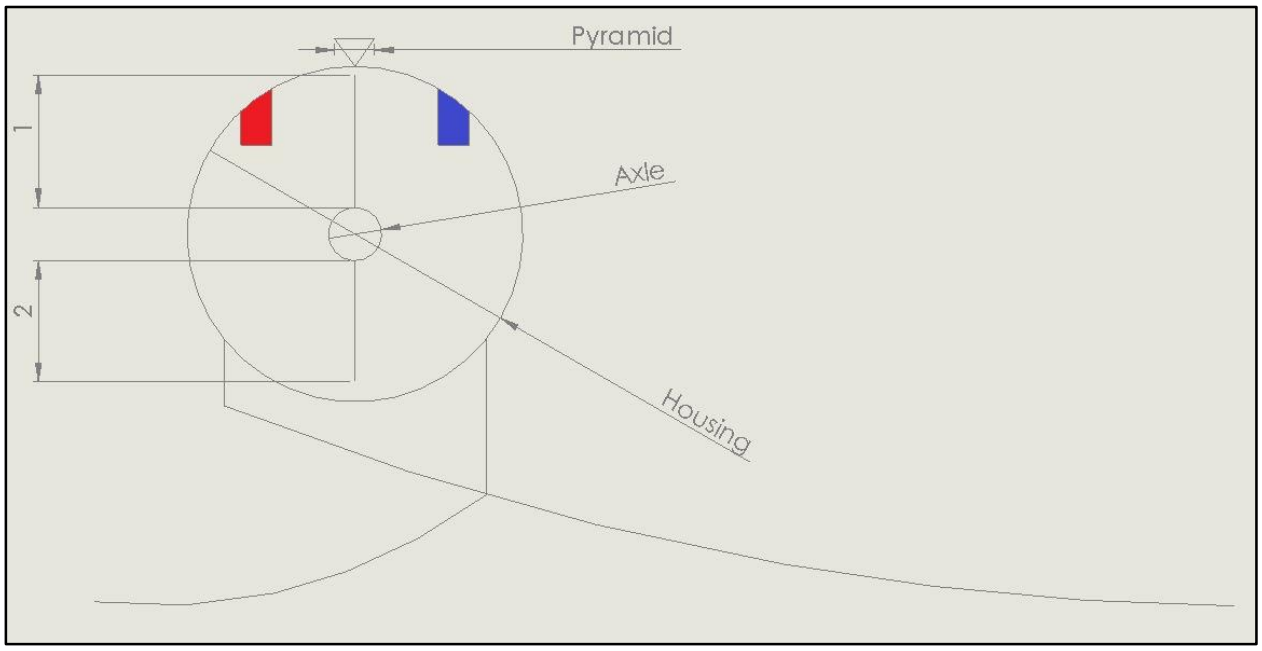

Figure 2.3: Design idea 3

The ankle design depicted in Figure 2.3 shows a rotary hydraulic actuator with two vanes, mounted on top a LP Vari-Flex foot plate, as in design 2. The pyramid is connected to the axle which moves freely over the housing. The vanes (1 & 2) are fixed to the axle and move with it. The inside of the housing is filled with oil which is moved around by the vanes. The main housing is split into two chambers. When the pyramid rotates clockwise over the housing, the oil is pushed out through the red opening and back in through the blue opening. There is a hydraulic hose connecting the red opening to the blue one. A bidirectional solenoid valve will be connected to the hose, controlling the flow between the openings. The solenoid valve will be controlled via an electric coil.

This design is simpler and increases manufacturability in the engineering machine shop. This gives it a slight advantage over the other two designs. It is also easily scalable, i.e. a bigger housing will result in a lower internal pressure as the vane size is directly proportional to the housing radius, and the internal pressure is proportional to the force applied to the oil by the vane. The overall pressure can therefore be calculated using equations 2.1 and 2.2

$$\sigma = \frac{F}{A} \tag{2.1}$$

where F is found from the generated torque at heel strike during level ground walking. The torque (T) will generate a maximum internal pressure,

$$P_{internal} = \frac{T}{\frac{L_{vane}}{2} * n * A_{vane}} \tag{2.2}$$

where L_{vane} is the length of the vane and n is the number of vanes. Therefore, by changing the inside diameter of the housing, the internal pressure will change, assuming the generated maximum torque remains constant.

This design was chosen as a proposed solution to the stair descent problem due to its simplicity and scalability. This makes it better suited to this project as it can more easily be machined using the equipment at hand.

2.4 Stair descent study using human subjects

In order to design a prosthetic foot which addresses the problem described in the problem statement, we need to understand the normal operation of the human ankle during stair descent. Many previous studies have addressed this problem [1, 13, 16, 22, and 33] and have provided

important information for the design criteria. A paper by Merkur Alimusaj et.al [1] describes a study done on 16 transtibial amputees looking at the kinematics and kinetics of stair descent. From this study we have a general plot of the ankle dorsiflexion/plantarflexion angles as well as maximum angles. Table 2-1 shows important data from this study.

Parameter	Sound side	Prosthetic side
Maximum Plantar flexion	17 ± 11	4 ± 3
Maximum Dorsiflexion	39 ± 4	15 ± 6

Table 2-1: Ankle angles during stairs descent found in [1]

Table 2-1 gives us important values for transtibial amputees which are useful during the design process. Similar values are reported for transtibials by Sinitski et al. [33]. The problem with the papers found on this subject is the lack of transfemoral amputee data aside from one study [16] which only describes similar values as table 1 from a one-step stair descent but no additional data for complete staircases. Another problem is the controlled environment, as in the described transtibial study above, a five step staircase is used in a controlled laboratory environment. Due to these issues, it was decided to conduct a small study to get data in "real-life" situations. In order to acquire this data, a portable gait analysis equipment, made by Xsens, was used.

2.4.1 Xsens gait analysis equipment

The gold standard in gait analysis are optical motion capture systems. Such systems use infrared cameras along with reflective markers to compute the position of each marker in space. Cameras are often set up in a circular parameter around the area where the gait analysis is performed. Although this system is the most accurate it is big and expensive. Optical motion capture is often

coupled with a load cell to record ground reaction forces and thereby get accurate kinetic data along with the kinematic data but this is also an option in the Xsens system.

Figure 2.4: Gait analysis laboratory with an optical measurement system.
Image taken from: http://runblogger.com/2013/10/my-running-gait-analysis-at-spaulding.html

The equipment chosen for this study is the Xsens Mvn Biomech gait analysis suit. The Xsens suit consists of small IMU (Inertial Measurement Unit) sensors placed at specific places on the body. This system is composed of 17 IMU´s called MTx inertial tracker. 11 are for the upper body, 7 for the lower body, and 1 is for backup. All tracker data is sent to a pc via wireless transmitters and the post processing of the kinematic data is performed in the included software package.

Figure 2.5: XSENS system and included software package.
Image taken from http://wwww.est-kl.com/it/products/motion-tracking/xsens/mvn-biomech-awinda.html

Xsens Mvn Biomech is designed specifically with biomechanical research in mind. Reliability, accuracy, and data transfer speed as well as a sophisticated biomechanical model are among the advantages the system offers [2].

Figure 2.6: Xsens MTx tracker
Image taken from: https://www.xsens.com/products/mtx/

Each MTx tracker is composed of a tri-axial accelerometer, tri-axial gyroscope, and a magnetometer. Each tracker provides three degrees of freedom in orientation tracking. In order to get six degrees of freedom position tracking, three DOF linear acceleration tracking and three DOF angular velocity tracking, gyroscope integration is required as well as double integration of accelerometer signal, at each time step. Angles can be computed from the gyroscope by integrating them over time. Sensor signals are transformed into a global reference frame. Quaternions are used to compute the angular velocity in the global frame

$$\dot{q^{GS}} = \frac{1}{2} q_t^{GS} \otimes \Omega_t \tag{2.3}$$

Where q_t^{GS} is the quaternion describing the rotation from the sensor reference frame (S) to the global reference frame (G) [2]. This is equivalent to a rotation matrix but quaternions are used as they can offer computational and data handling advantages and can be more numerically stable when computing 3D orientation [11]. Ω_t is the quaternion representation of the angular velocity at time t [2, 3]. The rotation quaternion can then be used to compute the acceleration in the global frame using equation 2.4

$$a_t^G - g^G = q_t^{GS} \otimes (a_t^s - g^s) \otimes q_t^{GS^*} \tag{2.4}$$

It is now possible to remove the gravitational component from the acceleration and compute the global position [2]

$$\ddot{P}^G = a_t^G \tag{2.5}$$

From the computations above, we can apply the position data and angles to body segments using a biomechanical model. In order to get an accurate analysis, the setup process of the gait analysis system involves a fast and easy calibration process. After the trackers have been placed on the correct places on the test subject, tracker location is measured as well as limb length and anatomical landmarks. Finally, the test subject is asked to stand still while calibration is being processed. The calibration process uses equation 2.6. Rotation from sensor to body segment,q^{BS}, is found by matching the sensor orientation in the global, q^{GS} , frame with the known calibration orientation of the segments, q^{GB} [2].

$$q^{GB} = q^{GS} \otimes q^{BS} \tag{2.6}$$

Using the known lengths between trackers, as well as knowing the position of the subject during calibration, correct tracker positions can be computed by the MVN software. Finally, to ensure minimum errors, the magnetometer in the trackers is used to minimize rotation errors and gravity measurements from the accelerometers are used to minimize integration errors and drift by providing inclination stability [2, 3]. Errors in the Xsens system are still greater than in the optical motion capture. Average errors in angles are about 3° [10] which is higher than in optical motion capture but ease of use and mobility made the Xsens system ideal for this study and as the results of this study compared well with the values in Table 2-1, errors were deemed minimal. Errors increase with faster movements [10] and since no fast movements were recorded in this study we assume no greater errors than the average.

2.4.2 Human subject stair descent study

2.4.2.1 Participants

The study was conducted in the gait lab at Össur Inc. in Reykjavik, Iceland. The gait lab engineer gave a short training course on setup process and calibration. A total of three participants were analyzed, two transfemoral amputees and one able-bodied individual. Transfemoral amputees were high active and classified as K4 amputees. The K4 classification definition is given below, taken from [4]

"K-Level 4: Has the ability or potential for prosthetic ambulation that exceeds basic ambulation skills, exhibiting high impact, stress, or energy levels. Typical of the prosthetic demands of the child, active adult, or athlete."

Amputees used their own prostheses in order to mimic their normal gait. Both subjects had been using their prostheses for more than a year and were very familiar with how they work. Subject 1 used a glass fiber modular socket (MSS), a Rheo 3 microprocessor knee, and a Vari-Flex carbon

foot, all made by Össur Inc. The Rheo 3 microprocessor knee allow users to ambulate stairs and rough terrain using a magnetorheological actuator controlled using artificial intelligence. The actuator includes 63 blades separated by magnetorheological fluid. The metal particles in the fluid line up and create friction between the blades when a magnetic field is created by a coil in the center of the actuator. This brakes the knee joint allowing the user to walk down stairs step over step in a safe and controlled manner.

Subject 2 used a laminated socket made by glass fiber and polyurethane, a Powerknee motorized knee, and a Vari-Flex carbon foot. The Powerknee is a motor-powered prosthetic knee. It has a brushless dc motor that produces 96Nm of torque to compensate for the lost muscle power of the amputated leg. It is controlled using accelerometers, gyroscopes, load cell, torque sensor, and artificial intelligence to mimic natural gait.

Subject 3 was an able bodied individual and was analyzed as a control subject to have a proper comparison for the amputee data.

2.4.2.2 Protocol

Subjects were fitted with the Xsens suit, calibration was performed, and all measurements were taken to ensure the most accurate analysis possible. Subjects were then given 5-10 minutes to get used to wearing the suit and walking in it. Prosthetic alignment was checked on the amputees to make sure that everything was comfortable and aligned according to manufacturer's recommendations. The gait analysis process involved walking down two sets of stairs. Each subject walked up and down the stairs until two successful walks had been performed on each staircase.

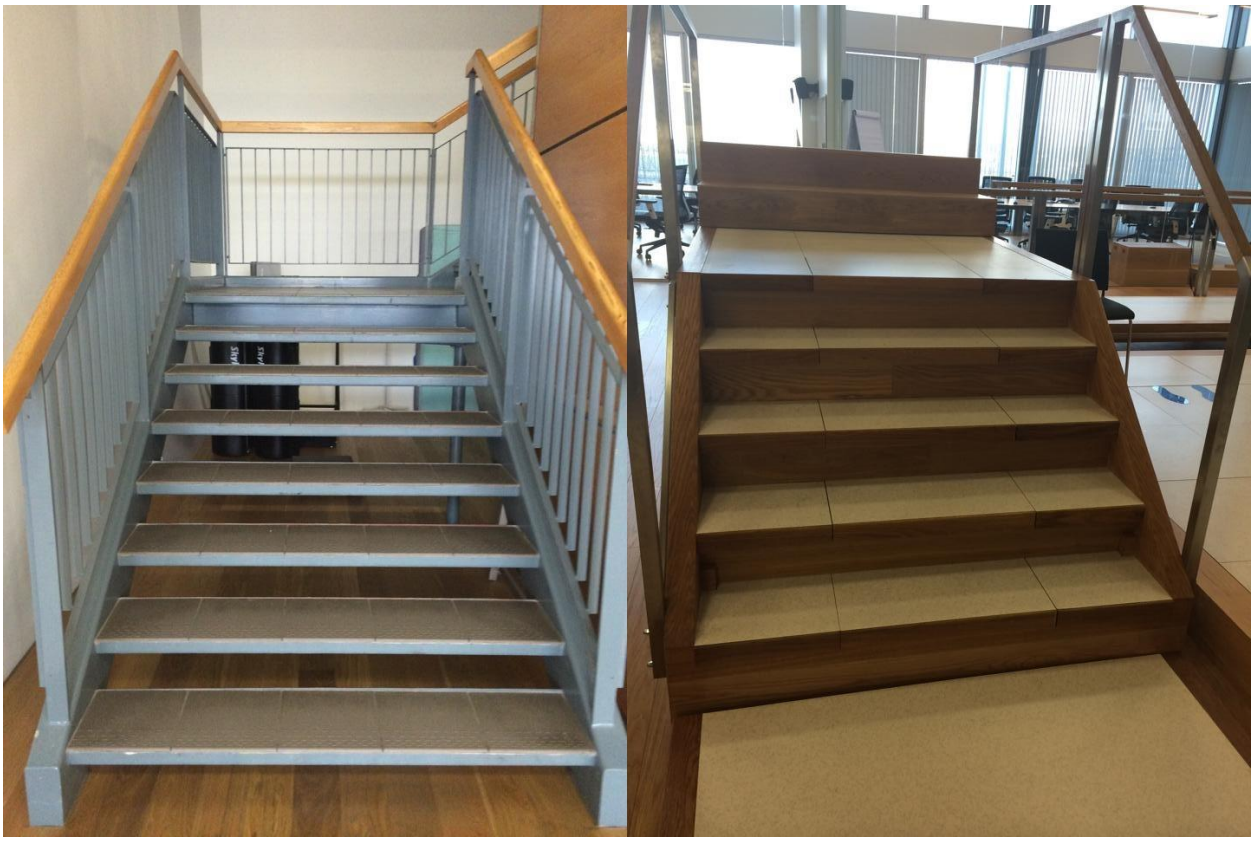

Figure 2.7: Staircase 1 on the left and staircase 2 on the right

Amputees had no skin breakdown or any other stump issues before starting this trial and no pain or discomfort was present at the time of the study. Each subject walked down the stairs without any specific instructions. They were asked to walk "normally" and could use a handrail if they wanted to as well as no specification was made on which leg to start the descent with. Amputees always started each run with placing the prosthetic side down into the first step as that was the most comfortable and normal way to ascend stairs for them.

Because Subject 2 had a motor-powered prostheses, both stair descent and ascent was analyzed but for this project, only the stair descent data was used. The stairs ascent data may be useful at a later date if the designed ankle will be modified to account for stair ascent as well.

Figure 2.7 shows both stairs used in this trial. Both stairs are built according to European standards but staircase 2 is in the maximum of those standards. Stairs 1 have 180mm height between steps but stairs 2 have a 220mm height between steps which is the maximum allowed height according to the standards [5].

No force plate was used in this trial as the kinetic data was not necessary for this study. Future studies might want to include a force plate to evaluate the load distribution and impact forces and compare the effect of using the designed ankle in this project to a standard carbon fiber foot.

2.4.2.3 Data analysis

The data from the stair descent study was analyzed using both the Xsens software and Matlab. During a gait analysis trial, all sensor data from the MTx IMU is transferred wirelessly to a computer. The Xsens software processes the data and computes position and angles from the inertial data using the equations above.

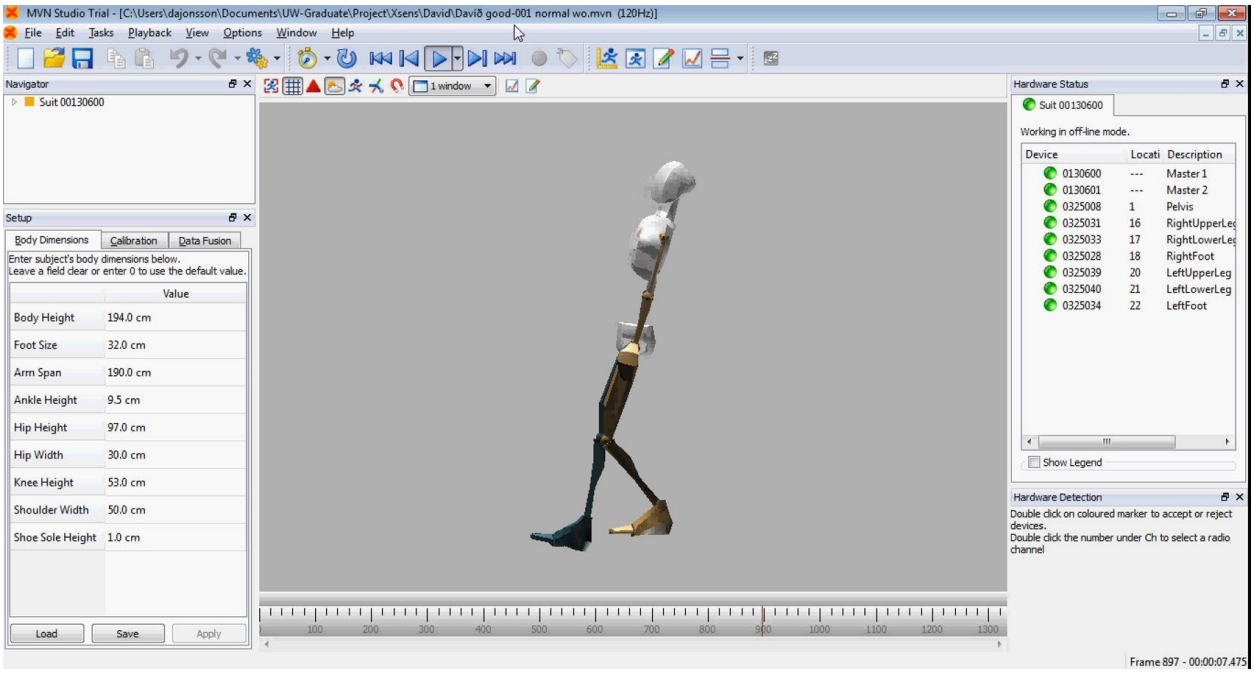

Figure 2.8: XSENS gait analysis software MVN studio

The data was then exported from the Xsens software, to an .xml file which is composed of all angle data, acceleration, velocity, and position data. A Matlab GUI (graphical user interface) program was written to analyze the data in Matlab. As Matlab has great computational power and provides the ability to process the data in any way easily, that program was chosen for this analysis. The Matlab program imports the .xml file and then converts it into a map data structure for fast lookup. The program then gives the user simple intuitive way of visualizing the data by plotting it.

The user imports the .xml file into the program using a simple button. The program prompts the user for the location of the file and provides the user with options of plotting joint angles or segment acceleration, velocity, angular acceleration, angular velocity, and position. As all the data from the sensors is in 3D, the plotting planes are divided according to biomechanical standards. These planes are Sagittal, Transverse, and Coronal and they divide the body according to Figure 2.9, in this study we are only interested in joint angles in the sagittal plane.

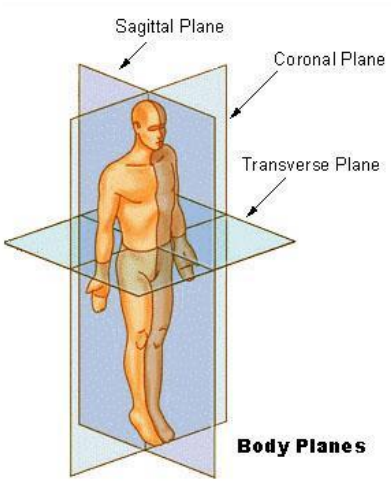

Figure 2.9: Body planes
Image taken from: http://speedendurance.com/wp-content/uploads/2011/11/3D-body-planes-200.jpg

The Matlab program also allows the user to save the plot data for additional analyzes and manual computations. This was added for easier data processing by exporting the plot data along with the time data to a .mat file which could then be read back into Matlab as an array and further processed.

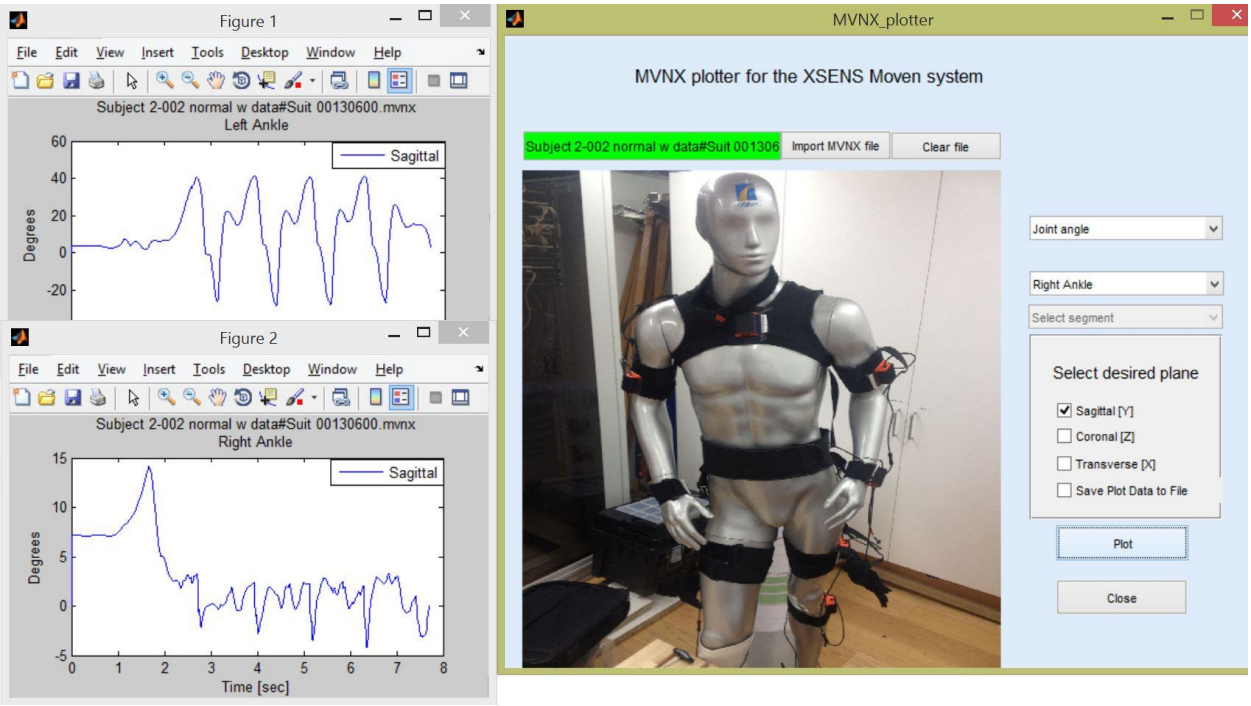

Figure 2.10: Matlab GUI Program created for data processing

Figure 2.10 displays the Matlab program. The picture in the program is the Xsens suit used in this study. The plots are given the same title as the name of the imported file and below that is a separate title with the name of the joint or segment that was chosen for the plot. The Y-axis of the plot has the plot variable and the X-axis displays the time in seconds.

2.4.2.4 Study results

All data was recorded using maximum refresh rate, 120Hz, to catch every movement, and to avoid undersampling errors. This refresh rate is much higher than was necessary but since each stair descent trial was short the amount of collected data was not too important as processing speed was not vital and it was considered better to have too much data than too little.

Each gait trial was imported into the Matlab program described above and saved into .mat files. Files that were of interest were mainly the joint angles of the sound side ankle. A short script was written to import all .mat files for each subject and analyze each step separately. Figure 2.11 shows one trial for subject 1 exported from XSENS Mvn studio and imported into the GUI Matlab program.

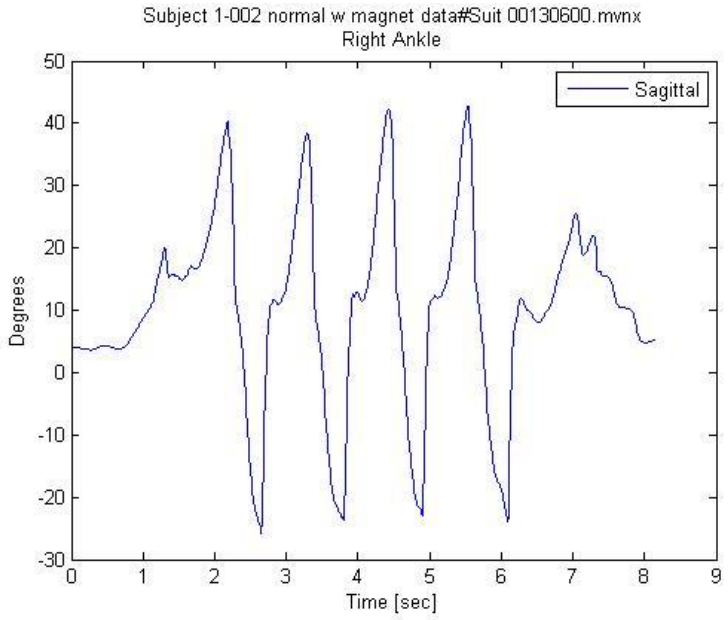

Figure 2.11: Ankle joint angle for subject 1 during one stair descent trial plotted by the GUI Matlab program

Figure 2.10 displays the ankle joint angle during one stair descent trial. The Xsens software sets the calibration joint as 0°. That means that 0° is the joint angle when the subject stands straight with arms down the sides, this will be considered our reference point in this study. Figure 2.12 shows how the ankle joint is measured, θ_1 shows the definition of the ankle joint. Clockwise movement (foot dorsiflexion) is positive and counterclockwise (foot plantar flexion) is negative.

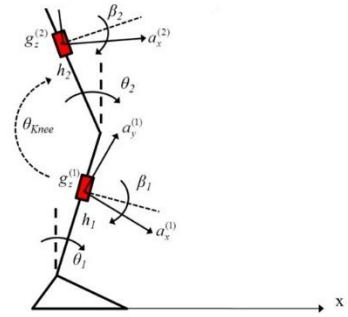

Figure 2.12: Ankle joint definition

Image taken from: [31]

During post processing in Matlab, only full steps were measured. In Figure 2.10 the first step was excluded as well as the last one, only the three steps in the middle (seconds 2.5-6) were measured. Each step was put into a matrix were each row was one step. Because all steps varied slightly in time duration, all steps were interpolated to match the longest step. An average step was then found and one standard deviation was also computed using equation 2.6

$$SD = \sqrt{\frac{\sum_{i=1}^{n}(x_i - \bar{x})^2}{n-1}} \tag{2.6}$$

$\bar{x}$ is the average value and n the number of steps. Table 2-2 shows the height and age of each subject

	Height [cm]	Age [Years]
Subject 1	180	35
Subject 2	194	27
Subject 3	160	25

Table 2-2: Age and height of study subjects

Subject 1

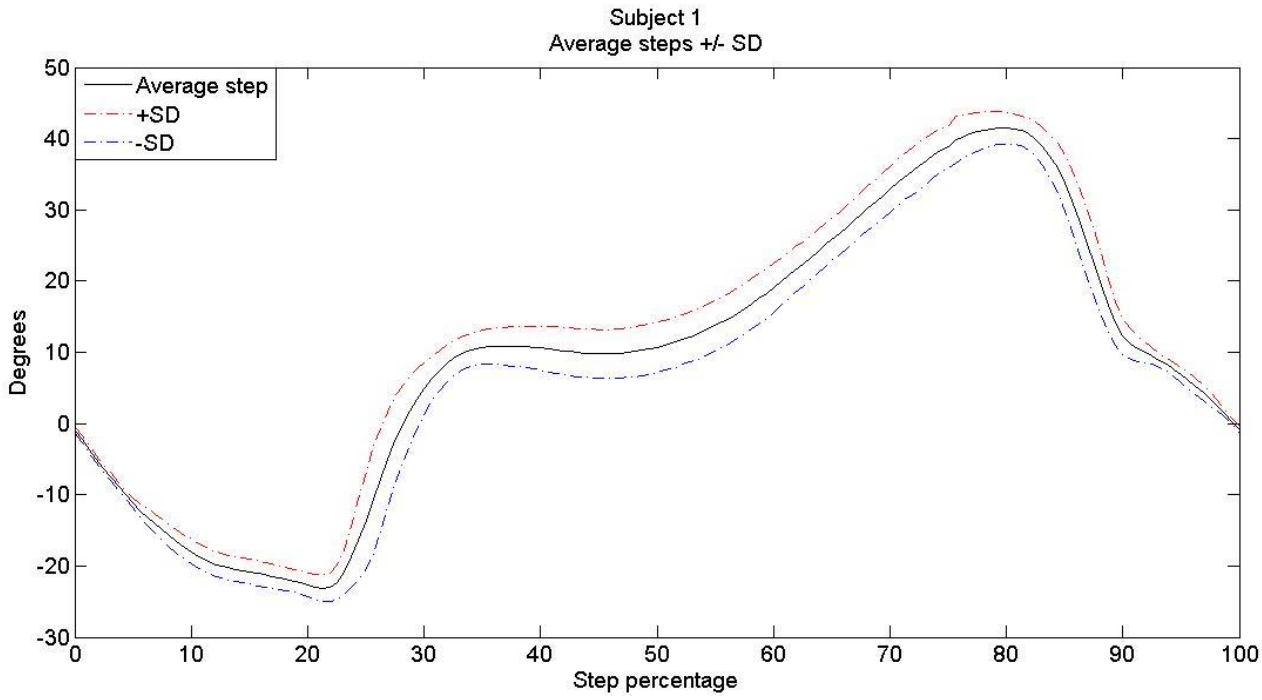

Figure 2.13: Subject 1 Average stair descent step for sound side ankle joint

Figure 2.13 shows the sound side ankle motion for subject 1 during the stair descent trials. The results in Figure 2.13 were computed from 9 complete steps taken on both stairs. There is not much variation in the steps as is seen by how closely the standard deviation follows the average line. The first 20% of the step shows the swing phase. During this time the ankle has a plantar flexion ~23°. Stance phase is between 20% - 80%. During this time the shank moves over the ankle and around 50% the subjects center of mass is directly over the ankle which explains the saddle point. As the subject moves into the next step on the prosthetic side, the ankle goes into further dorsiflexion in order to keep the sound side flat on the step. Maximum dorsiflexion of ~41° occurs just before toe off at 80%.

Subject 2

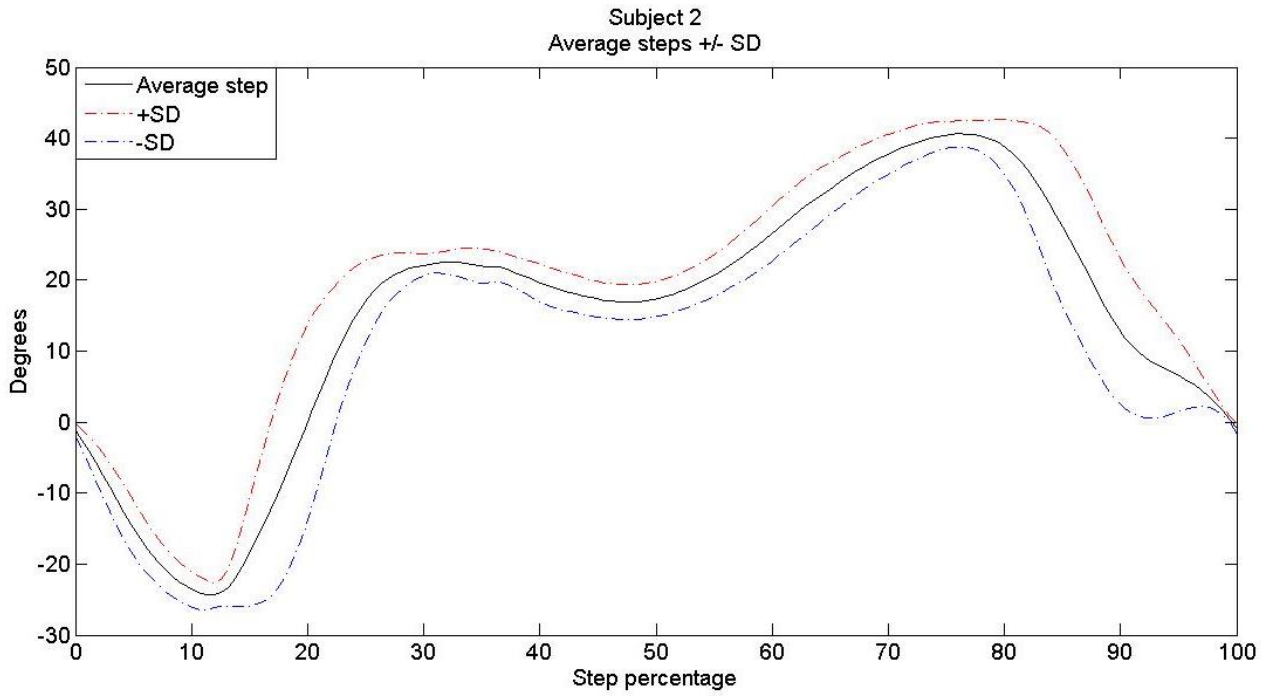

Figure 2.14: Subject 1 Average stair descent step for sound side ankle joint

Figure 2.14 shows the sound side ankle motion for subject 2 during the stair descent trials. The results in Figure 2.14 were computed from 10 complete steps taken on both stairs. We see more variation for subject 2 than for subject 1. The overall shape of the average line is similar but the stance phase starts sooner at around 12% and toe off occurs around 76%. The standard deviation does not follow the average line as closely as for subject 1. The saddle point reaches 20° which is 10° more than subject 1 but the maximum dorsiflexion is the same as for subject 1 (~41°). The greater variation for subject 2 could indicate a greater stability for subject 1. The greater stability could arise from more training and muscle control but it could also be the result of the different prosthetic knees chosen by the subjects. The difference does not affect design of the prosthetic ankle in this project as the maximum dorsiflexion is the same and the overall shape of the average line is similar.

Subject 3 (Control subject)

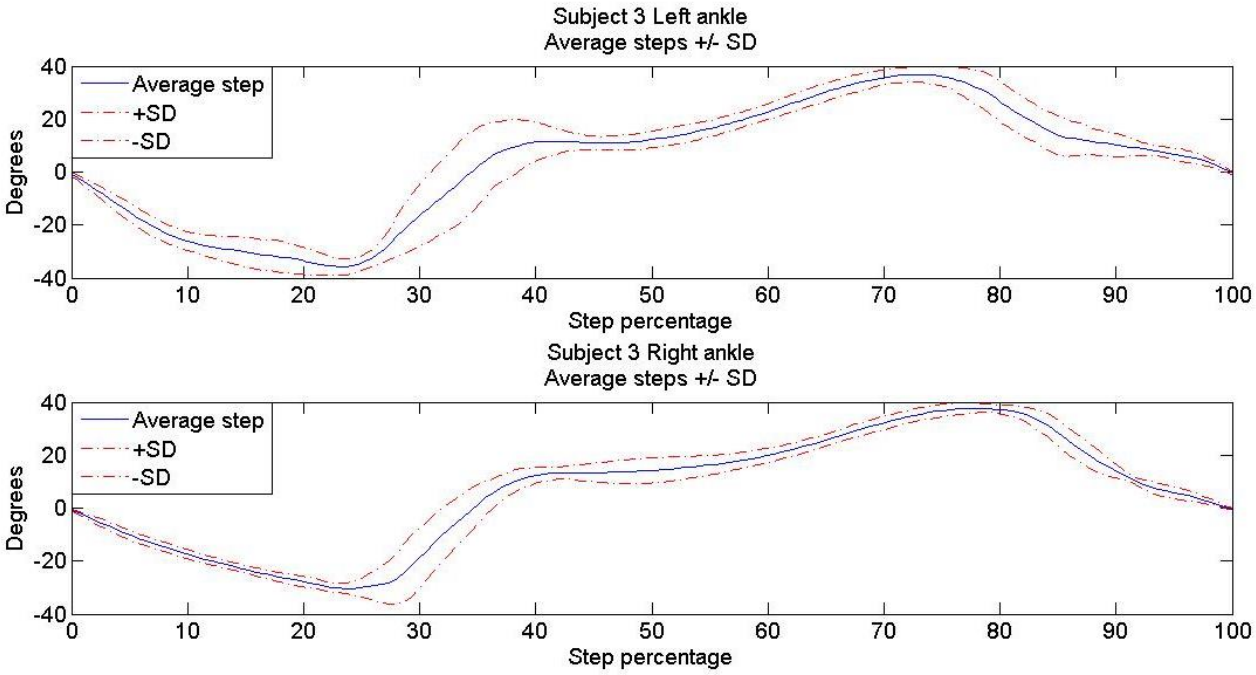

Figure 2.15: Subject 3 Average stair descent step for both ankle joints

Figure 2.15 shows the ankle motion of both ankles for subject 3 during the stair descent trials. The results in Figure 2.15 were computed from complete steps taken on both stairs, 9 taken on the left ankle, and 8 taken on the right. We see in Figure 2.15 that subject 3 is more stable on the right ankle but both ankles show the same general shape as we see for the other 2 subjects. The maximum value for the average line is ~36° for the left ankle and ~37° for the right ankle. This is slightly lower than the other 2 subjects. We see a similar pattern in Sinitski et al. [33], i.e. that able-bodied have a slightly smaller range-of-motion than amputees have on the intact side, but it could also be explained by the lower height of subject 3. One standard deviation from the average line does reach 40° for both ankles. We see that the overall ankle motion is similar for all subjects and no different ankle motion is noticeable for the prosthetic users. Subject 3 does stay in swing phase longer and stance phase occurs later and the initial plantarflexion seems more controlled and

slower. This can be explained by the prosthetic knee, during stair descent on the prosthetic knee it provides resistance but the user has little control. Step-over-step prosthetic stair descent has been compared to controlled falling down the step as was discussed in chapter 1. The sound side therefore has to be quick to catch the user on the next step. This is the only noticeable difference between the amputees and the control subject. During stance phase there is little difference and that is the important part of this project.

2.5 Solidworks design process

The actual design in Solidworks is the final part of the design process. The design criteria for the drawings were based on the stair descent study and available off-the-shelf components.

2.5.1 Design criteria

Weight limit for the prosthetic ankle was chosen to be 90kg. This number was chosen from the weight of the designer as the ankle was to be built and tested by the designer at a later date. A 90kg person will generate a maximum moment of ~135Nm over the ankle [22, 30, 34]. The range of motion for the ankle was chosen to be 35°. In order for the user to get the prosthetic foot off the step at the end of stance it is important to flex the knee slightly more. Since most prosthetic knees are passive (no motor power) we need to flex the carbon foot-plate to get a small push, from the energy return of the carbon, to flex the knee. This is the reason 35° was chosen as the maximum range of motion so that ~5° flexion will be reached by the carbon fiber foot plate at the end of stance phase. Future testing will then determine if this is sufficient flexion or if greater flexion is necessary.

Internal pressure was chosen based on available off-the-shelf valves. It was decided to go with an off-the-shelf valve to limit cost and manufacturing time of the first prototype. The design presented is easily scalable and a custom valve was therefore left for a later date, a design is proposed for a

custom valve in chapter 3. A solenoid valve was chosen that runs on 12V. The valve, depicted in Figure 2.16, is sold by McMaster-Carr and has a product number: 5077T144.

Figure 2.16: Solenoid valve sold by McMaster-Carr, product number: 5077T144

image taken from: http://www.mcmaster.com/#catalog/121/497/=x4w1ms

The chosen valve is a solenoid valve and does not offer simple solution for flow control. Therefore an absolute maximum range of motion was chosen and a mechanical stop is incorporated into the ankle design. The solenoid valve has a maximum pressure drop of 2.7579 MPa (400 psi), is fully submersible, height: 1 5/8" (41.275mm), and length: 2 ¾" 69.85mm long. Pipe size is ¼" (NPT).

Arduino was chosen as the microprocessor for this ankle due to price, availability, processing speed, and simplicity. As the ankle was not machined and tested all programming discussion will be left for the future work section in chapter 3.

2.5.2 Solidwork drawings

In this section the new ankle design will be presented. Each part/assembly will be covered and discussed as well as material selection for each component. Detailed assembly instruction is

covered in appendix A and all 2D work drawings are shown in appendix B including dimensions and all necessary information for machining the ankle.

2.5.2.1 Axle and vane

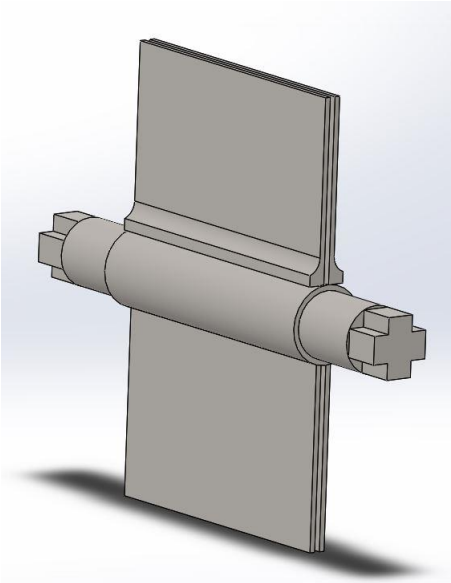

Figure 2.17: Axle and vane design

Figure 2.17 shows the axle and vane design. The vane slides into the axle to minimize material waste during machining. The vane has a groove around its edges where a rubber seal goes in. This seal will be cut out or 3D printed from a rubbery material. The material for the axle and vane was chosen to be stainless steel due to the high forces acting on the assembly. The axle will mainly be subject to shear stress during walking. During running the ground reaction forces are approx. 300% of bodyweight [7] so we assume a maximum impact force of 2700N which will result in ~24MPa of average shear stress on the axle when using equation 2.7.

$$\tau = \frac{V}{A} = \frac{F}{A} \tag{2.7}$$

$$\tau_{max} = \frac{16T}{\pi d^3} \tag{2.8}$$

The maximum stress from the torsion can be found from equation 2.8 [7]. The design criteria assumes a torque T=135Nm and the diameter of the axle is 12mm. Maximum shear is therefore ~400MPa which is distributed on both sides of the axle, resulting in ~200MPa on each side. Stainless steel would be sufficient for a prototype but a more aggressive design use would require titanium or high strength stainless steel.

A more thorough finite element evaluation is given in chapter 3.

2.5.2.2 Main housing

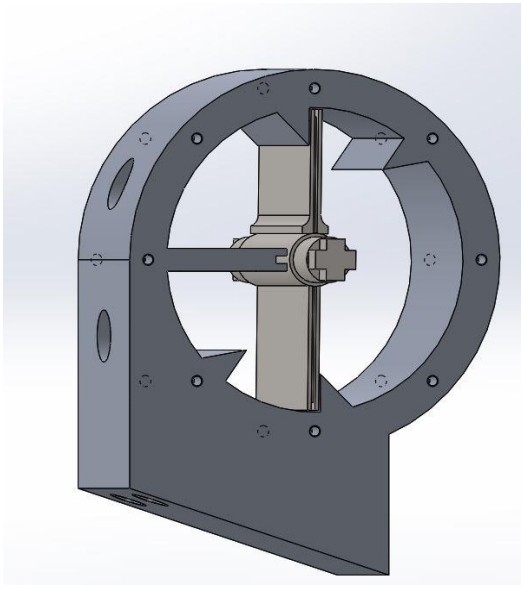

Figure 2.18: Main housing

The main housing, shown in Figure 2.18, houses the vane and is filled completely with oil. There are two openings on the left side where the solenoid valve is connected. In between the openings

there is a separator which separates the main housing into two chambers. The separator has a groove similar to the vane where a rubbery seal will be inserted and lie tightly up against the axle. The bottom of the main housing has an angle of 18° to fit nicely on top of the foot plate and will be tightened using M10 bolts. Inside the main housing the vanes are allowed 35° of motion which is restricted by the small walls that the vanes lie up against in Figure 2.18. The main housing will be machined from 7075 aluminum.

2.5.2.3 Sides

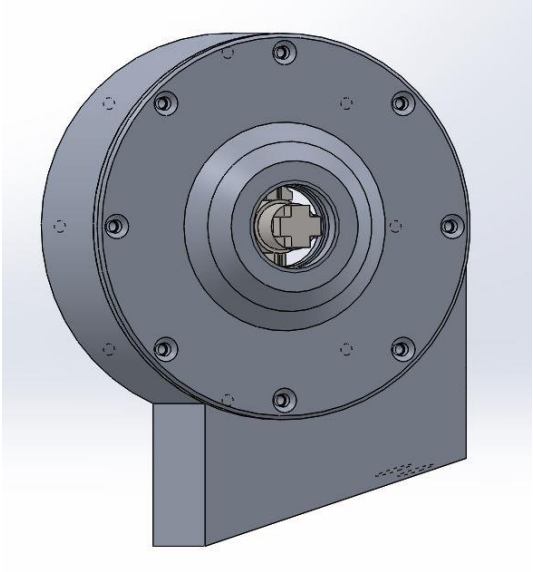

Figure 2.19: Sides of main housing

The sides, shown in Figure 2.19, close the main housing. They are fastened using 8 countersunk screws evenly placed around the edges. A bushing can be placed between the side and the main housing if required for better sealing. In the center of the side is a threaded hole where the axle goes through. A roller bearing fits in the hole to hold the axle in place. The bearing is not visible in Figure 2.19 but can be seen in the assembly instructions found in appendix A. The sides will be machined from 7075 aluminum.

2.5.2.4 Sealing screws

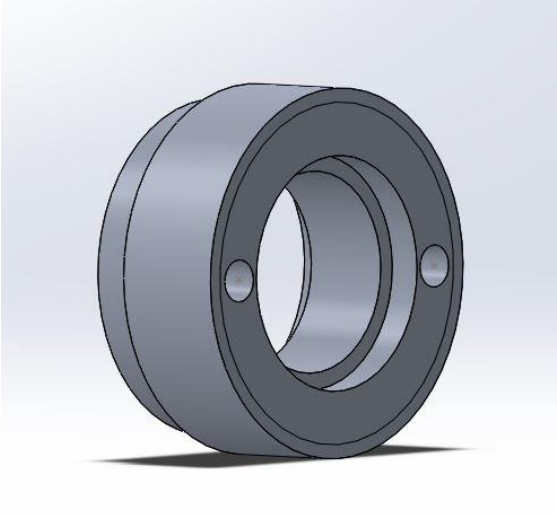

Figure 2.20: Sealing screw

The sealing screw, shown in Figure 2.20, goes into the hole on the housing side and screws up against the bearing. The purpose of the sealing screw is to seal the edges of the bearing to maintain a complete seal of the ankle. There are two holes on the front of the sealing screw which are intended for screwing it into place. Figure 2.21 shows a section view of the ankle with the sealing screw in place.

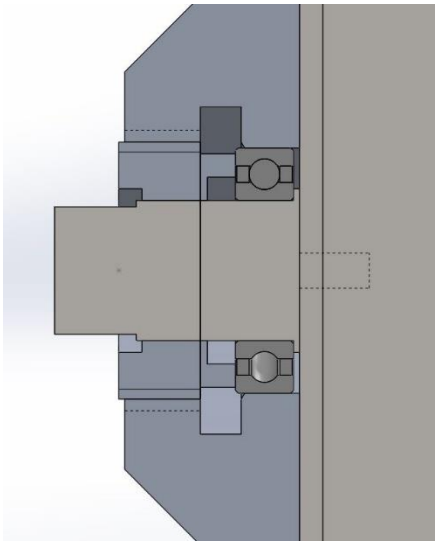

Figure 2.21 - Section view of sealing screw

Figure 2.21 shows a section view of one side. The bearing is held in place using a pre-loaded assembly method. The axle has a slightly greater diameter on the right side of the bearing. This prevents the bearing from moving into the main housing. The sealing screw screws up against the outer edge of the bearing causing a pre-load which holds the bearing in place. On the sealing screw we see a gap up against the axle and also up against the side. These gaps are designed for O-rings that seal the edges of the bearing when the sealing screw is fastened. The sealing screw will be machined from 7075 aluminum.

2.5.2.5 Pyramid and load bearing sides

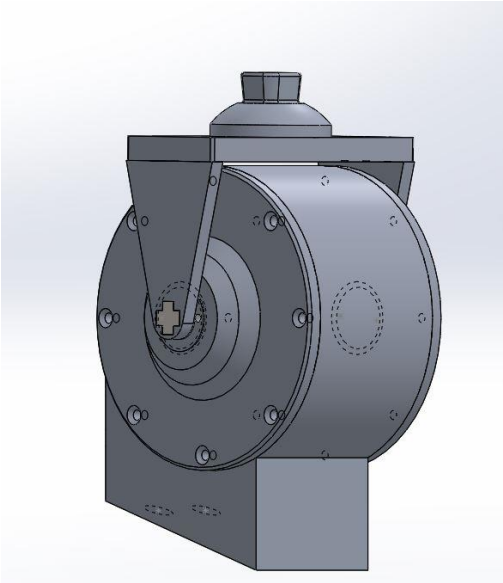

Figure 2.22: Load bearing sides and mounting pyramid

Figure 2.22 shows the final part of the ankle design, the load bearing sides and the pyramid. The load bearing sides are connected to the axle on one side and to a plate on the other. On top of the plate is a standard size pyramid, an industry standard for prosthetics. The load bearing sides and pyramid will be machined from 7075 aluminum for the prototype but for more aggressive use the pyramid and load bearing sides will need to be made from either stainless steel or titanium for additional user safety and durability.

The overall build height of the ankle is ~1cm taller than a standard Vari-flex and can easily be tested by most transfemoral amputees.

Finally, Figure 2.23 shows the complete prosthetic ankle with the carbon foot plate, the foot plate is a rough drawing for visualization and not a realistic replication of the actual foot plate.

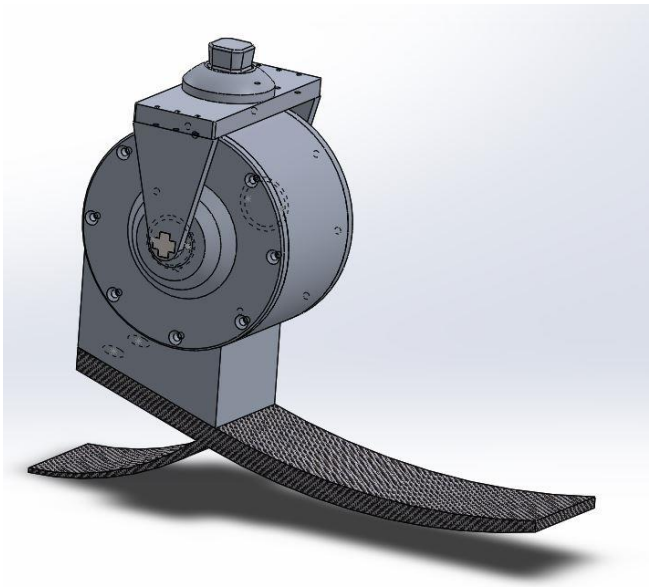

Figure 2.23: Fully assembled prosthetic ankle

The only thing missing in Figure 2.23 is the extension spring that moves the pyramid back to the original position after each stair descent step. A spiral torsion spring was intended for the extension spring but due to design changes when adding the sealing screw, a spiral torsion spring could no longer fit. Adding an extension spring inside the main housing would be ideal but during the early stages of the design phase, no additional extension spring design was considered and therefore there was no more time to redesign the extension spring. For this design, an extension spring would therefore need to be attached to the back of the main housing and onto the base plate under the pyramid. The benefits of the spiral torsion spring over the extension spring is the constant force offered in torsion springs. Further discussion of future extension spring improvements are included in chapter 3.

2.5.3 How does the ankle work?

The ankle will have an inertial sensory system for gait recognition. When it senses a vertical displacement equivalent to stair descent it will open the solenoid valve. When the user loads the foot, the vanes will push the oil through the solenoid valve and thus allowing 35° of dorsiflexion. After 35°, the carbon foot will compress by approximately 5° which will provide the push off which flexes the knee enough to move the foot off the step and down into the next step. During the swing phase, the extension spring will plantar flex the foot and move the pyramid into the initial position to prepare for the next step. At the end of the stair descent, the inertial sensors will recognize the gait change and close the solenoid valve when the foot is in swing phase to ensure that the foot is fully plantar flexed.

With improved programming and valve control the ankle could also be used for improved incline walking. Walking up an incline puts greater strains on a transfemoral amputee's hip as the knee stays fully extended and as the amputee moves over the foot, only the toe touches the ground. By allowing dorsiflexion, the entire foot would stay on the ground reducing hip moment as the carbon foot would no longer be generating knee extension moment which works against the forward momentum of the amputee.

3 Evaluation and future work

This chapter is split into two sections. The former section presents conclusions from a finite element analysis performed on the ankle design. Finite element analysis was performed both using Solidworks' built in function as well as using the finite element software ANSYS. Results from this analysis is presented and used to verify material selections from chapter 2.

The latter presents necessary future work needed before the ankle can be tested and manufactured. Aside from future work discussions, it also provides suggested design changes as well as suggestions on programming the ankle function.

3.1 Finite element analysis (FEA)

A finite element analysis was performed to evaluate whether the designed ankle could withstand the expected loads during human testing. Although most of the design process was based on hand calculations described in chapter 2, during the design process preliminary analysis was also done on load bearing components using Solidworks' built in FEA analysis. Further analysis on the full assembly was performed using ANSYS when the design was complete.

There were two elements of interest during the FEA, total displacement and the Von-Mises stress criteria. Displacement was chosen to verify the ankles rigidity. Too much motion in the ankle during level ground walking could cause instability for the amputee. The Von-Mises stress criteria was decided for a simple validation of the material selection. It is the most widely used yield theory for ductile material. It computes a single scalar stress value from a complex stress state which can easily be compared to a materials yield strength [28].

3.1.1 Solidworks FEA

The selected material for the following parts is 7075-T6 aluminum alloy.

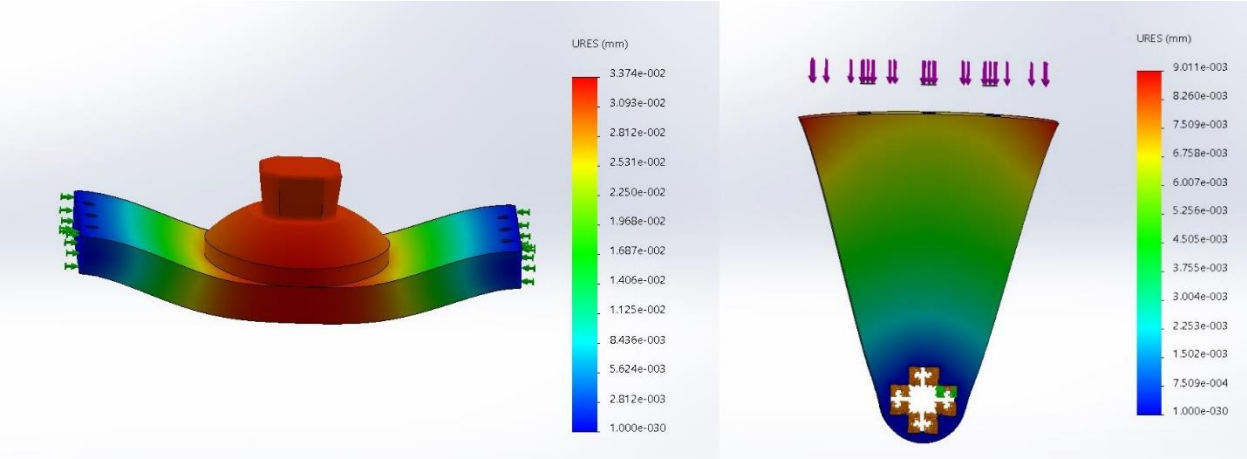

Figure 3.1: Solidworks FEA analysis of load bearing components. Total displacement

The FEA tool in Solidworks generated the mesh automatically during analysis. We see from Figure 3.1 that the total displacement for the pyramid is at the center as expected. It is only 0.03374mm which is well within all boundaries. The only risk was that the pyramid would deflect so much that it touches the main housing but this is far away from that. Displacement on the load bearing sides are practically zero and need no further investigation.

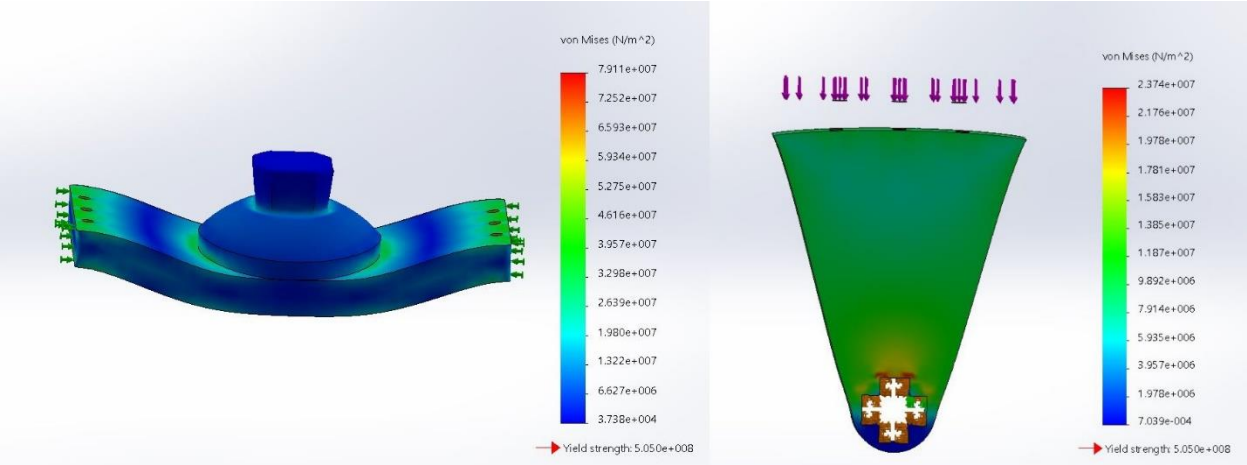

Figure 3.2: Solidworks FEA analysis of load bearing components. Von-Mises stress

There is not much information we can gather from the stress analysis on these individual parts other than that they will not yield under the current loads. The values presented are in Pascal

(N/m^2) and they are much lower than the yield strength for the given material. This analysis is not a perfect replica of the subjected loads as the pyramid will not be fixed on the sides but by screws on top and the load bearing side will have a plate connected to the top which will cause slightly different forces. This is not of any concern, as the stresses are far from yield and the fixed supports are similar enough to present similar loads as human testing.

3.1.2 ANSYS FEA

ANSYS was used to perform a more thorough finite element analysis on the complete assembly. The analysis was limited to a static analysis on the ankle design. The static analysis was considered the most important before the ankle is built and tested on a human subject. Both Von-Mises stresses and displacement are presented but displacement may not be accurate as component material selection in ANSYS was limited to the included materials which did not include the materials selected in chapter 2. This was not considered a problem as the stresses were the desired results of the ANSYS analysis. Von-Mises stresses will be the key-results of this analysis as they will be used to either verify material selections done in chapter 2 or to propose different materials.

Two scenarios were analyzed, static force and static moment.

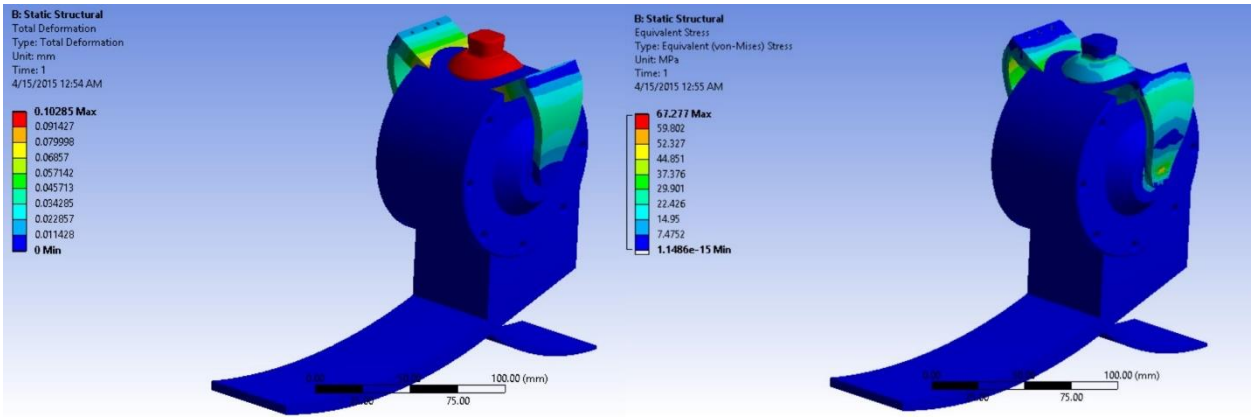

Figure 3.3: Static force analysis in ANSYS

Figure 3.3 displays the results of a static force, 2700N, acting vertically on the pyramid. We see from the figure that the displacement is greater than in Solidworks. That could result both from a different material selection or because the analysis is performed on the complete assembly. The displacement is still relatively small, only 0.1mm, and the pyramid is far from colliding with the main housing. Looking at the right image in Figure 3.3 we see the stresses resulting from the vertical force. All the stresses acting on the load bearing sides are below 50MPa, much lower than the yield strength of the chosen material for this part. The pyramid plate has even lower stresses. The highest stresses are expected at the axle due to its smaller area than the load bearing sides. Figure 3.4 shows a closer look at the stresses on the axle. We see greater forces but not significantly, all forces are well below the yield stress. We see a maximum force at the edges of the axle end but only of ~67MPa. Vertical impact forces will therefore not be a problem for the design and no need is to reevaluate the material selection from chapter 2 because of the vertical impact forces.

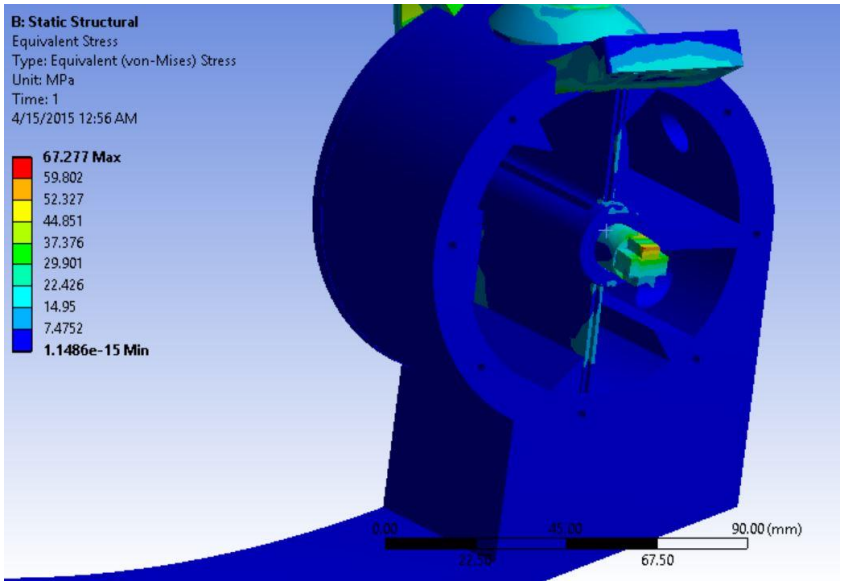

Figure 3.4: Figure 3.3: Static force analysis in ANSYS, axle close-up

One more FEA study was performed on the proposed design. Figure 3.5 shows the results of the last analysis. A 135Nm moment was generated over the axle to analyze how the load bearing sides will move and to see the how the vanes will deform.

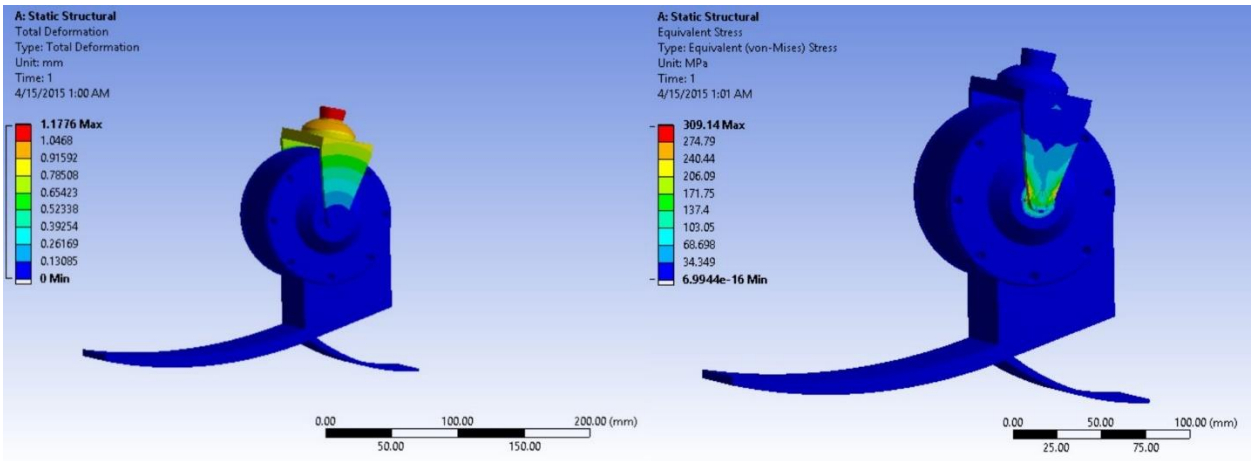

Figure 3.5: Static torque analysis in ANSYS

There is a much greater deflection from the generated moment over the axle. This is expected as 135Nm of torque is equivalent to the output torque of a small car. Relative to the displacement from the vertical force, this is ~11 times greater which puts the amount of torque into some perspective. As was mentioned above though, the material selection in ANSYS is not accurate and so the deflection will be lower if the proper material is selected.

Looking at the Von-Mises stresses we notice that the scale goes to ~310. This maximum value happens at a small point on a sharp corner and is likely a singular stress point. The stresses on the load-bearing sides are most below 150MPa and go to ~200MPa in the two yellow areas. For a prototype this should not cause any issues for the chosen material in chapter 2 although the 7075 aluminum alloy might need to be heat treated for additional strength if the prototype were to be tested extensively.

Due to the relatively large radius of the main house, the vane will be subject to the greatest stresses as it is long and thin. Figure 3.6 shows the stress distribution on the vane when subject to 135Nm of torque. The size of the mesh was reduced for the vane to minimize the risk of singular stresses on the sharp edges of the vane. We see a singular stress point at the corner where the vane slides into the axle. At the corner there is a peak stress which we can ignore as it is most likely a singular point and will not result in the vane failing under load. We do see much greater average stresses than in the load bearing sides. We see up to ~350MPa stresses acting on the vane close to the axle. This high stress will break standard stainless steel and it would therefore be better to choose a cold rolled stainless steel that has a yield strength >400MPa. With a redesign of the vane with a greater thickness close to the axle and thinner near the main housing, the stresses will be lower; however, this design was favored due to less waste during machining and thus a cold rolled stainless steel is preferable over a different design.

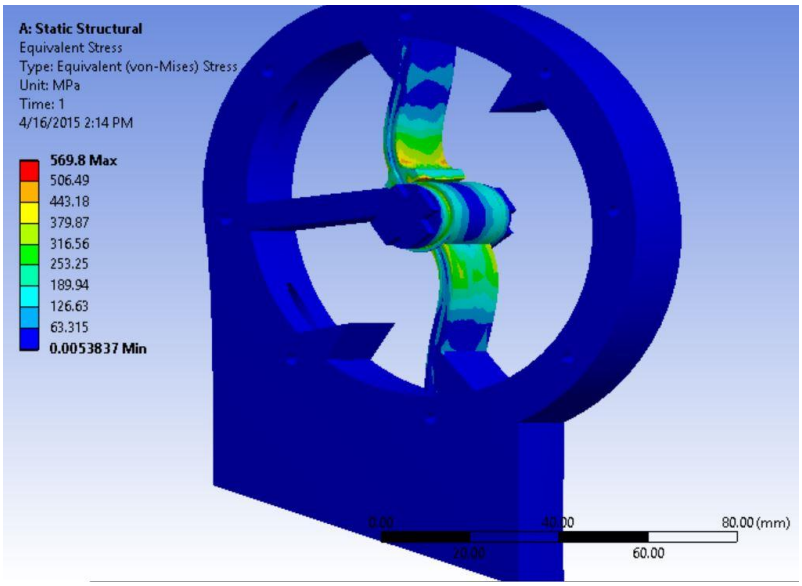

Figure 3.6: Stresses on the vane during torque analysis

3.1.3 Summary and future analysis

Finite element analysis has been presented for individual components as well as the full assembly. Von-Mises stresses support the material selection from chapter 2 but small changes are encouraged especially, for the vane; even though the material would be the same it needs to be cold rolled for additional strength.

The presented analysis should be sufficient for the prototype but it is far from being comprehensive. Additional analysis should be performed before extensive human testing takes place. Of course one could spend months analyzing various design considerations, using ANSYS, and overanalyzing the design would be a waste of time so a few analysis are suggested that are considered most important. It might be interesting to perform a fluid analysis to see the oil flow during movement of the ankle. Such an analysis could support some redesign of the chamber holes on the main housing. Some fatigue analysis would be good as well. There is not necessarily a need for such an analysis for a first prototype but for later designs it will be required.

A dynamic analysis could also be done using ANSYS as well as a non-linear analysis. This could be useful for analyzing the carbon fiber foot-plate. Finally it might be interesting to see how temperature changes will affect the function of the ankle. Such an analysis could affect the choice of oil used inside the main housing but it might also be better to perform such an analysis on the physical prototype rather than in ANSYS.

3.2 Future work

The design proposed in this thesis should help improve some of the problems transfemoral amputees have during stair descent. It would be foolish though to assume it would fix all issues instantly, or that a first design could not be made better. The design proposed is a very good starting point to what might be a great transfemoral prosthetic ankle but some future work is required to

improve the design. In this section a few important improvements are proposed but this section is in no way a comprehensive list of the required work. With further work on the design more areas might appear that require additional improvements.

3.2.1 Prototype building

The most obvious work required is making a prototype of the design. Machining the components and assembling the ankle would be the first task. The design is complete and along with the 2D work drawings in appendix B there is no additional work required before it is possible to build the ankle. Appendix C lists the off-the-shelf components necessary for the design along with the product numbers from McMaster-Carr.

After the first prototype has been built, mechanical testing should be performed. Stress testing the design to make sure it will hold a human subject would be required to prevent any injuries during human testing. Mechanical testing is a vital part of medical product design and before the commercial product is ready fatigue testing will be required using mechanical testing equipment. This involves cyclic loading of the ankle using both a vertical force as well as torque.

During the mechanical testing of the prototype, oil selection would be performed. The oil will be selected based on the viscosity. The ideal oil should be viscous enough so that it will not leak past the vane-seals, causing creeping of the ankle, but it should not be so viscous that all rotary movements will be too slow. The oil selection will be a vital part of the design and will require extensive testing to optimize.

3.2.2 Programming the ankle

Before the prototype can be properly tested on a human subject some programming work is required. For the first prototype, the programming work does not need to be extensive or complicated. The only requirement for this prototype is to recognize stairs descent. When stairs

descent is recognized the valve is opened to allow the oil to flow between the two chambers and allow the ankle to move in dorsiflexion.

The electronics chosen for the prototype were an Arduino board which was chosen only for its simplicity. The simplest way to accomplish the task of stair recognition is to integrate an accelerometer's signal twice to get position data. A good way to do this is to use the trapezoidal method on the signal, equation 3.1. v_n is the velocity at the n_{th} timepoint, a is the accelerometer value, and Δt is the time-difference between the last measured value to the current value.

$$v_n = v_{n-1} + \int_{t_{n-1}}^{t_n} a(t)dt \approx v_{n-1} + \frac{1}{2}(a_{n-1} + a_n) * \Delta t \tag{3.1}$$

The issue with numerical integration are the round-off/truncation errors that can result in a significant drift. To minimize this drift it is useful to recognize heal strike (usually appears as spikes on the accelerometer data) and set the position to zero at that point. Using the computed position data it is possible to set a limit to ~10cm and whenever the vertical displacement exceeds this limit, a stair descent step is detected. When this has been achieved, human testing can be performed on the prototype.

If the valve were replaced with a custom design valve (A design is proposed below) that offers flow control, a different control scheme could be developed. Stair descent could still be recognized using double integration of an accelerometer but instead of just opening a valve, the resistance of the dorsiflexion in the ankle could be controlled by controlling the flow. A good way to control such a valve would be to look at the knee joint angle during stair descent and base the resistance of that value. If we take a look at some of the data collected from the stair descent study from chapter 2, Figure 3.7 displays the knee joint angle plotted as a function of the ankle angle for one

step, both for the intact limb and the prosthetic limb. Each figure used the average value of three complete steps for subject 1.

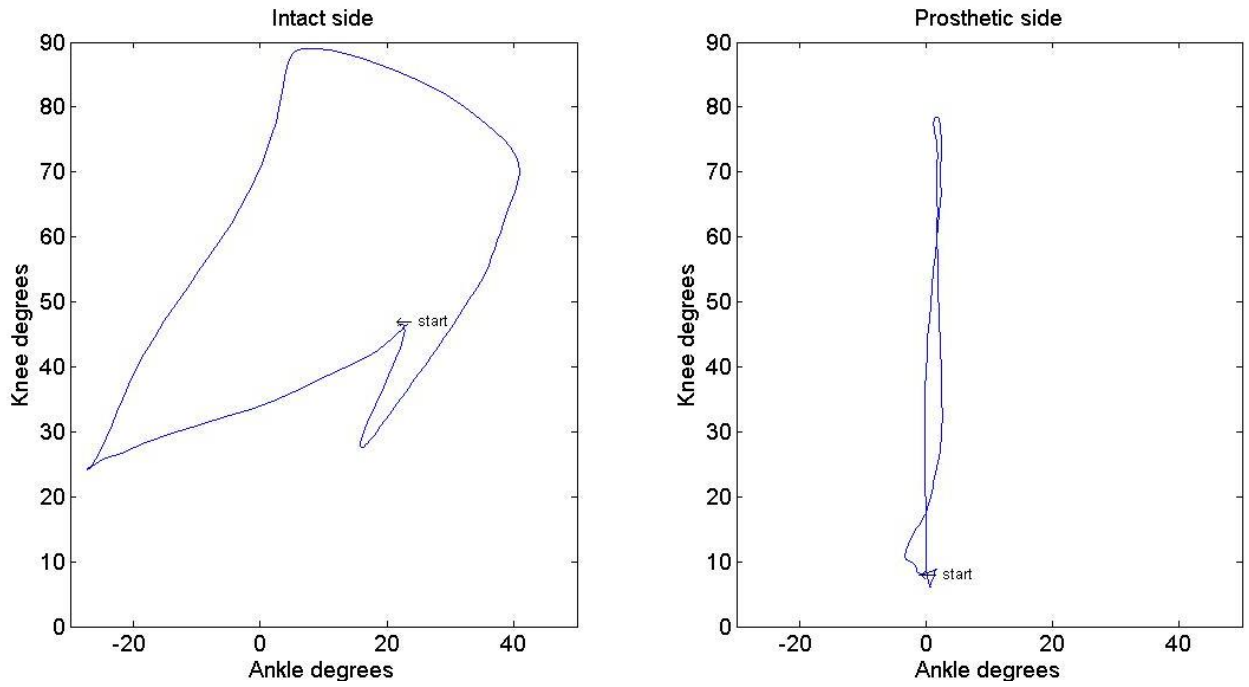

Figure 3.7: Knee angle as a function of ankle angle during stair descent of subject 1

In Figure 3.7 the starting points are marked on the graphs. It is interesting to see the ankle movement of the prosthetic side which ranges from ~-3° to ~2°. When looking at the intact side we travel from the start point and move to the right as the graph starts during stance phase. When the ankle is in the greatest plantarflexion (at the bottom left corner) the foot lands on the step. The knee then flexes slightly to dampen the impact. The starting point is at the maximum flexion of this dampening (stance flexion) before the knee starts extending again. After full knee extension, the knee then moves into controlled flexion and the ankle moves into dorsiflexion at the same time. Using this information along with an angle sensor for the ankle, a PID controller could be designed to control the ankle resistance such that this behavior could be replicated on the prosthetic side which is the aim of prosthetic feet, to mimic the sound side or even improve it.

Future improvements could also involve small dorsiflexion during level ground walking for additional toe clearance as well as incline walking but more advanced control system and algorithms are required for accurate sensing of all activities.

3.2.3 Reducing size

When it comes to prosthetics size really does matter and smaller is usually better than bigger. The designed ankle is of a reasonable size for fitting it to a transfemoral amputee but reducing the size means reduced weight which in turn reduces the amount of work it takes to move it during walking. The valve is the bottleneck of the design as it can only withstand <3MPa of pressure. To reduce the size of the ankle it is necessary to design a custom valve for the ankle that can withstand greater pressure. By increasing the allowed pressure inside the main housing the length of the vane can be reduced as per equation 2.2. This will also reduce the stresses acting on the vane near the axle and relief some of the yield strength requirements.

Figure 3.8 depicts a proposed valve design for the prosthetic ankle. The proposed design would provide better flow control and should be able to withstand greater pressures than a solenoid valve.

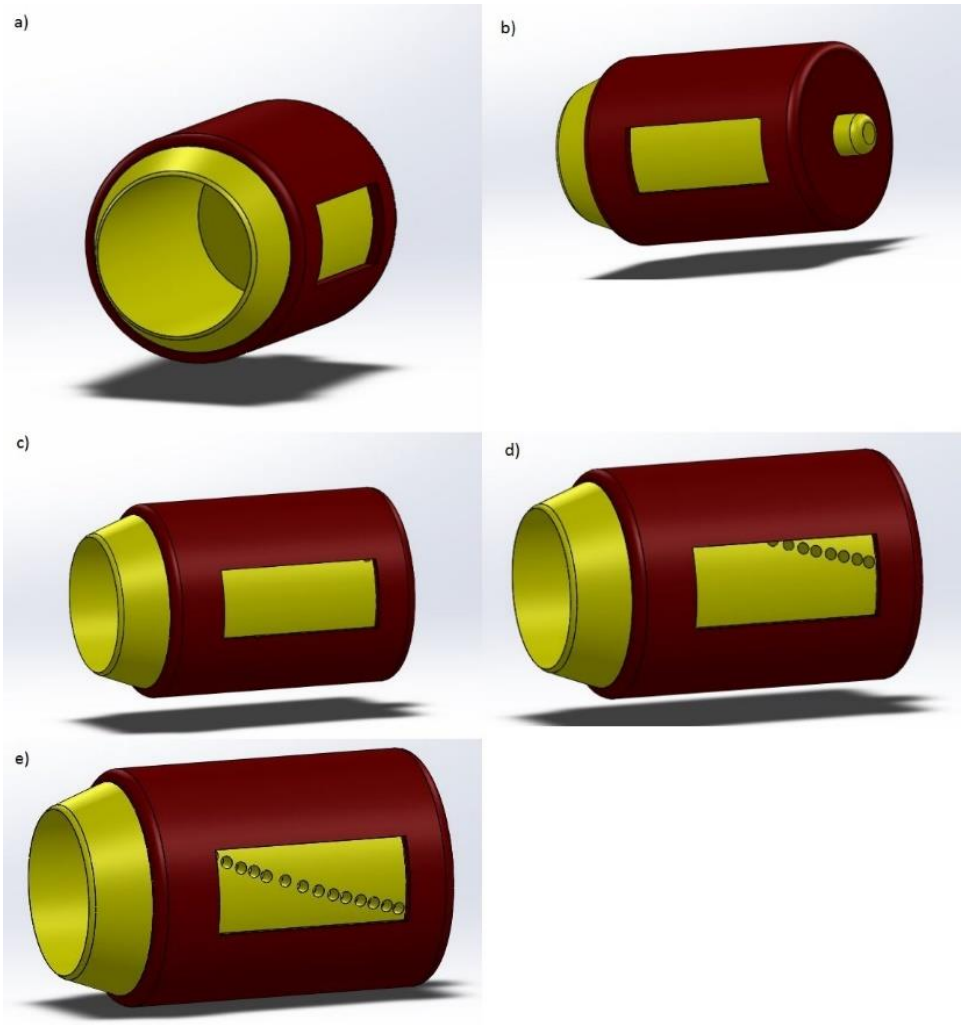

Figure 3.8: Proposed valve design

In Figure 3.8, a) & b) show both ends of the valve and the side. The valve consists of two components. The inside component (yellow) is open wide on one side and closed on the other side. From the closed side there is a small pin sticking out. On the side of the inside component are a series of small holes that go through the side of the component. The outside component (red) is a container for the inside component. On the side of the outer component is a rectangular window and on top is an opening for the small pin. Images c), d), and e) display the function of the valve. By turning the small pin the inside turns and by doing so the small holes on the side line up with

the window. The further you turn, the more holes appear until they reach from corner to corner along the diagonal of the window.

This valve would slide into the chamber separator on the main housing which would need to be redesigned to house the valve properly. The lower end would be placed into one chamber and the window on the side would be open into the other chamber. When no holes are visible in the window the valve would be closed. By turning the valve and exposing more holes the flow between chambers will increase. The top pin will stick out of the main housing and a small stepper motor will be connected to the pin. By controlling the stepper motor it would be easy to control the flow between the two chambers of the main housing and thus the resistance of the ankle.

The proposed design would of course need to be designed in more detail for proper sealing and control but it does provide a fairly simple way to fix a big problem.

3.2.4 Carbon foot plate

Improved design is required for the carbon foot plate that the ankle is mounted on. Although the LP Vari-Flex is a good prosthetic foot for level ground walking it was chosen primarily for its low build height. Due to this low build height it does not flex as much as larger carbon feet which offer a smoother, less firm, experience and better dynamics. The carbon foot for the designed ankle would therefore ideally be higher and have a shape that provided a smooth roll-over during walking, has a good range of motion, and provides a good energy return during toe-off.

3.2.5 Extension spring

As was mentioned in chapter 2 the extension spring design for the ankle is not ideal. The original design idea did not work because of sealing issues and unfortunately no other designs were considered. The current design, having the extension spring come from the rear and latch onto the pyramid plate, is not ideal as the spring force will be a function of the springs length, generating

greater force the further the user moves into dorsiflexion. A spiral torsion spring would be better, and was originally considered, due to its constant force. Designing a spiral torsion extension spring that fits inside the main housing would be ideal for functional and aesthetic reasons.

3.2.6 Future research

Due to the lack of published research, a lot is still unknown about transfemoral amputee stair descent gait. A few ideas are listed here below that would be most beneficial for future improvements to the presented ankle design.

Transfemoral amputee stair descent study: A study of the kinetics and kinematics during transfemoral amputee stair descent. A motion capture analysis study of stair descent on a full staircase, coupled with ground reaction forces, would be necessary for future designs. The study could be similar to the one presented in this thesis but with more subjects and maybe using optical motion capture for greater accuracy.

Foot placement study: No published studies were found on foot placement during stair descent. Is it difficult for transfemoral amputees to place their prosthetic foot repeatedly in the same way at the edge of the step? Furthermore, if they do have a problem with correct foot placement, are they at risk of missing the step when trying to place only the heel at the edge?

Risk of falling: Is there a significant increase in the risk of falling for transfemoral amputees? By placing the heel at the edge of the step, is it possible that the foot slides over the edge, causing a stumble or fall, and if so, how much greater is the risk compared to placing the entire foot on the step?

Intact ankle range of motion: As was mentioned in chapter 2, able bodied individuals have a slightly smaller range of motion than the intact ankle of transfemoral amputees during stair

descent. It would be both very informative, as well as useful, for future design improvements to know whether the amputees' intact ankle range of motion would revert back to normal when using the presented ankle. By measuring the amputees' range of motion before being fitted with the new ankle, and at certain intervals after being fitted (1 week, 1 month, 2 months etc.) we could see if wearing this ankle could improve this gait abnormality.

4 - Summary and Conclusion

This thesis has presented a detailed description of the design process for a prosthetic ankle that can improve stair descent gait for transfemoral amputees. The aim of the project was to better understand all the components involved in designing a prosthetic ankle. This process was listed in great detail, such that it could maybe help others as well with their designs as this process can be applied to other areas with minor modifications.

The first chapter describes the problem at hand. Transfemorals tend to place their heels on the edge of the step and "roll" over the edge of the step during stair descent. This causes increased loads on the intact limb, causing gait abnormality, and increases risk of falling compared to normal stair descent gait. A literature review was also completed, but limited research has been done on amputee stair descent gait and only one paper was found on transfemoral amputee stair descent gait.

The second chapter covers the entire design process. Starting with three different design ideas, one was chosen, based on the pros and cons of all the ideas. After choosing the best idea, all design criteria was decided. In order to properly generate the design criteria, more gait information was needed than what is provided in the one study described above. Therefore, a gait analysis study was performed using two transfemoral amputees and one able-bodied individual as a control subject. To record the gait an inertial sensor suit, produced by Xsens, was used. The recorded data

was imported into Matlab and analyzed. The results were used to generate the design criteria. Finally, the ankle was designed, and the design was presented.

The third chapter covered two topics. Firstly a finite element analysis was presented for the ankle design to verify that the ankle would be able to support a human subject. This analyses supported all material selection from chapter two with minor modifications. Secondly some future improvements were discussed. Some future design changes were proposed along, with some discussion about how to program the microprocessor for the prototype.

The designed ankle will contribute greatly to transfemoral amputee health. By better mimicking a natural stair descent gait the ankle will help reduce loads on the intact limb and likely reduce the risk of developing knee pain. It will also reduce the risk of falling by allowing the user to position a greater amount of the foot on the step. After incorporating the design improvements mentioned in chapter 3, especially the adjustable valve, the ankle will also aid lower k-level amputees with day-to-day activities. By allowing for dorsiflexion at toe-off during level ground walking it will reduce the risk of catching the toe during swing phase. It can also help incline walking by dorsiflexing the ankle to adapt to the inclination.

If the aim of a master's thesis is to deepen a student's understanding of his field, learn how to properly research specific areas, work independently, and to apply knowledge from his studies to successfully solve a problem, this thesis has to be considered a great success.

Bibliography

1. M. Alimusaj, L. Fradet, F. Braatz, H.J. Gerner, S.I. Wolf, “Kinematics and kinetics with an adaptive ankle foot system during stair ambulation of transtibial amputees”, Gait & Posture, 30, pp. 356-363. 2009

2. D. Roetenberg, H. Luinge, P. Slycke, “Xsens MVN: Full 6DOF Human Motion Tracking Using Miniature Inertial Sensors”, Xsens Technologies, April 2013

3. H. Luinge and P. Veltink, “Inclination measurement of human movement using a 3D accelerometer with autocalibration,” IEEE Transactions on Neural Systems & Rehabilitation Engineering, vol. 12, no. 1, pp. 112–121, 2004.

4. Weisstein, Eric W. "Quaternion." [Online]. Available: http://mathworld.wolfram.com/Quaternion.html

5. R.S. Gailey, K.E. Roach, B. Applegate, B. Cho, B. Cunniffe, S. Licht, M. Maguire, M.S. Nash, “The Amputee Mobility Predictor: An Instrument to Assess Determinants of the Lower-Limb Amputee’s Ability to Ambulate”. Arch Phys Med Rehabil, Vol 83, 2002.

6. “UK Building regulations 2010” [Online]. Available: https://www.gov.uk/government/uploads/system/uploads/attachment_data/file/8393/2077370.pdf

7. T.S. Keller, A .M. Weisberger, J.L. Ray, S.S. Hasan, R.G. Shiavi, D.M. Spengler. “Relationship between vertical ground reaction force and speed during walking, slow jogging, and running”. Clinical Biomechanics, Vol. 11, pp. 253-259, 1996.

8. James M. Gere, Barry J. Goodno (2009). *Mechanics of Materials*. Toronto, Canada: Cengage Learning. 227-229

9. “Vari-Flex” [Online]. Available: http://www.ossur.com/prosthetic-solutions/products/feet/feet/vari-flex

10. “LP Vari-Flex” [Online]. Available: http://www.ossur.com/prosthetic-solutions/products/feet/feet/lp-vari-flex

11. A. G. Cutti, A. Giovanardi, L. Rocchi, A. Davalli, “A simple test to assess the static and dynamic accuracy of an inertial sensors system for human movement analysis”. Preceedings of the 28th IEEE EMBS Annual International Conference, New York City, USA, Aug 30- Sept 3, pp. 5912-5915, 2006.

12. Jack B. Kuipers, “Quaternions and rotation sequences”, Geometry, Integrability and Quantization, Coral Press, pp. 127-143, September 1999.

13. O.S. Mian, J.M. Thom, M.V. Narici, V. Baltzopoulos, “Kinematics of stair descent in young and older adults and the impact of exercise training”, Gait & Posture, 25, pp. 9-17, 2007

14. F. Sup, H. A. Varol, J. Mitchell, T. J. Withrow, M. Goldfarb, “Preliminary evaluations of a self-contained anthropomorphic transfemoral prosthesis”. IEEE/ASME Transactions on mechatronics, Vol 14, no. 6, 2006.

15. M. D. Geil, “Energy storage and return in dynamic elastic response prosthetic feet”. Pediatric gait, 2000.

16. T. Schmalz, S. Blumentritt, B. Marx, “Biomechanical analysis of stair ambulation in lower limb amputees” *Gait & Posture,* vol. 25, pp. 267-278, 2007.

17. D. C. Norvell, J. M. Czerniecki, G. E. Reiber, C. Maynard, J. A. Pecoraro, N. S. Weiss, “The prevalence of knee pain and symptomatic knee osteoarthritis among veteran traumatic amputees and nonamputees”. Arch Phys Med Rehabil, Vol 86, 2005.

18. “Motionfoot MX manual” [Online]. Available: http://www.centri.se/images/Product_pictures/Motion_Foot/Motion-Foot-MX-Manual.pdf

19. “Kinterra brochure” [Online]. Available: http://www.freedom-innovations.com/wp-content/uploads/2014/10/Kinterra-brochure1.pdf

20. H. M. Herr, A. M. Grabowski, “Bionic ankle-foot prosthesis normalizes walking gait for persons with leg amputation”. Proc. R. Soc. B, 279. pp. 457-464, 2012.

21. S. K. Au, H. M. Herr, “Powered ankle-foot prosthesis”. IEEE Robotics & Automation Magazine, pp. 52-59, 2008.

22. S. Au, M. Berniker, H. Herr, “Powered ankle-foot prosthesis to assist level-ground and stair-descent gaits”. Neural Networks, 21, pp. 654-666, 2008.

23. “Proprio Foot” [Online]. Available: http://assets.ossur.com/lisalib/getfile.aspx?itemid=6979

24. “Odyssey” [Online]. Available: http://www.springactive.com/odyssey.php

25. R. D. Bellman, M. A. Holgate, T. G. Sugar, “Sparky 3: Design of an active robotic ankle prosthesis with two actuated degrees of freedom using regenerative kinetics”. Proceedings of the 2nd Biennial IEEE/RAS-EMBS International Conference on Biomedical Robotics and Biomechatronics, pp. 511-516, 2008.

26. “Élan flyer” [Online]. Available: http://www.endolite.com/catalogue/feet/elan/downloads/en_US/Elan%20Flyer%20US3.pdf
27. “Élan product information” [Online]. Available: http://www.accessprosthetics.com/pdfs/products/elan-product-information.pdf

28. Richard G. Budynas, J. Keith Nisbett (2011). *Shigley’s Mechanical Engineering Design*. New York, USA: McGraw-Hill. 219-225.

29. M. Asghar Bhatti (2005). *Fundamental Finite Element Analysis and Applications*. New Jersey, USA: John Wiley & Sons.

30. David A. Winter (1987). *The Biomechanics and Motor Control of Human Gait.* Ontario, Canada: University of Waterloo Press.

31. A. Caroselli, F. Bagalà, A. Cappello, “Quasi-Real Time Estimation of Angular Kinematics Using Single-Axis Accelerometers”. Sensors, 13, pp. 918-937, 2013.

32. “Ottobock C-Leg Prosthesis - 15 Years of Supporting Amputees” [Online]. Available: http://www.disabled-world.com/assistivedevices/prostheses/c-leg-prosthesis.php

33. E. H. Sinitski, A. H. Hansen, J. M. Wilken, “Biomechanics of the ankle-foot system during stair ambulation: Implications for design of advanced ankle-foot prosthesis”. Journal of Biomechanics, pp. 588-594, 2012.

34. A. Protopapadaki, W. I. Drechsler, M. C. Cramp, F. J. Coutts, O. M. Scott, “Hip, knee, ankle kinematics and kinetics during stair ascent and descent in healthy young individuals”. Clinical Biomechanics, pp. 203-210, 2007.

Appendix A-Assembly instructions

1. Assemble one side to main housing using m3-screws	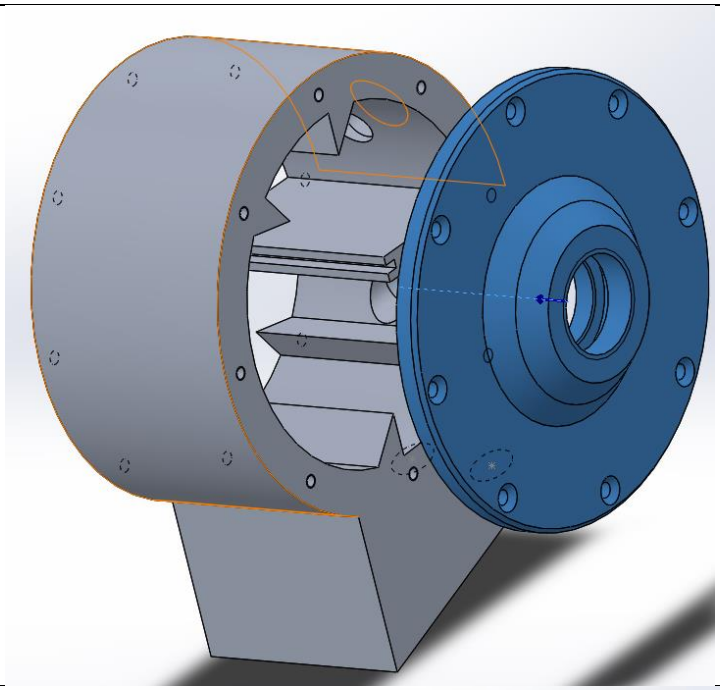
2. Glue gasket seals under the wings of the vane 3. Slide bearing on the right side of the axle until up to bearing seat 4. Add seals to vane-edges and then slide it inside the axle 5. Insert vane assembly into main housing	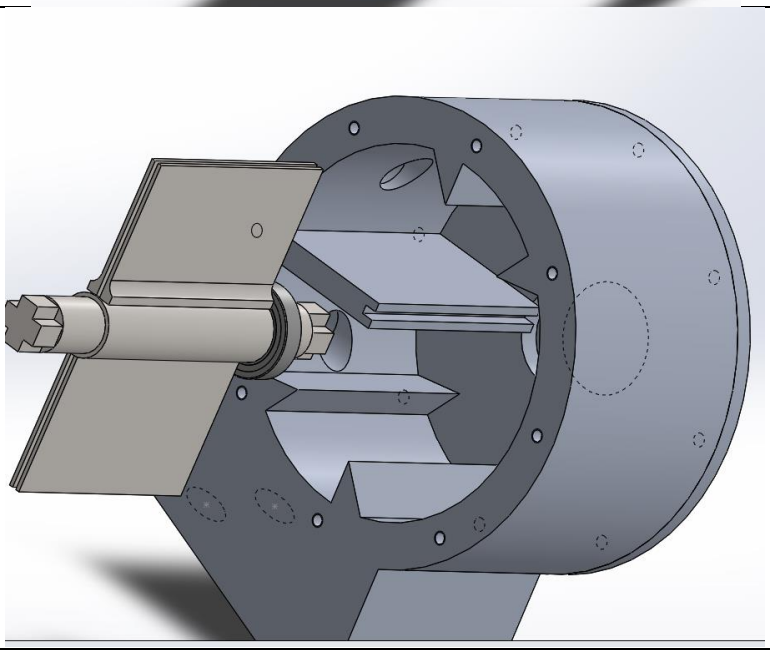

6. Assemble O-rings to right end on shaft so it sits against the bearing 7. Assemble O-ring to the outside groove of the sealing screw 8. Screw sealing screw into the side, tighten firmly, and fasten using epoxy glue.	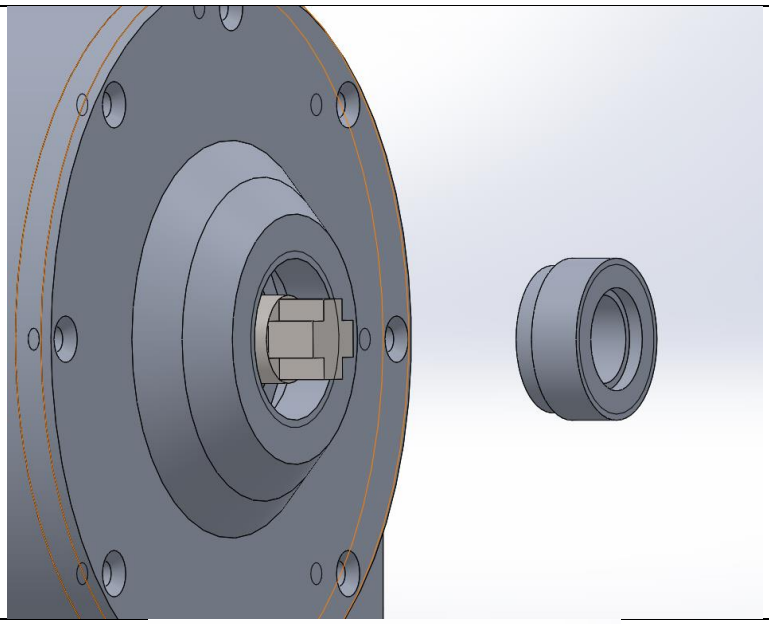
9. Attach hydraulic hoses and solenoid valve to the back of the main housing	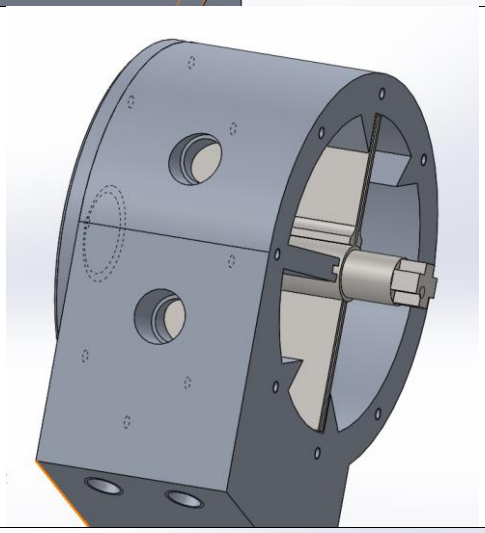
10. In a vise, create pulling on the axle on the assembled side to compress seals and seal off the side. Then fill the inside housing with oil	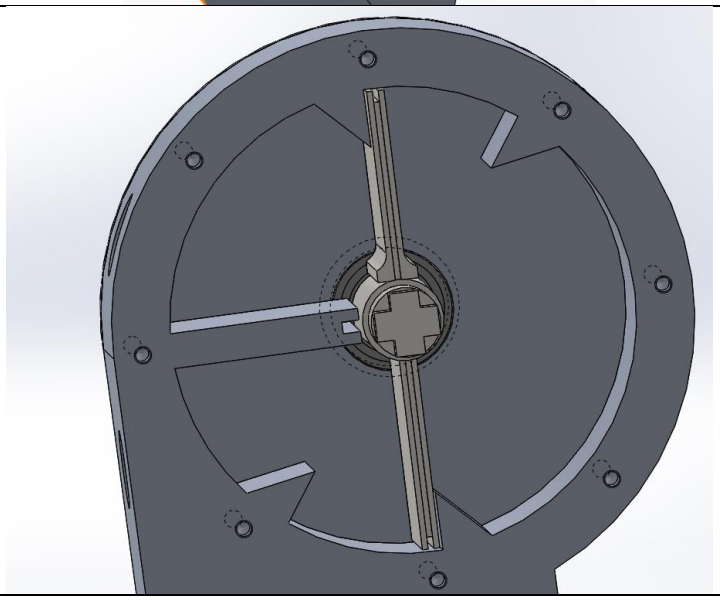

11. Add bearing to the axle and then assemble the side as instructed in step 1	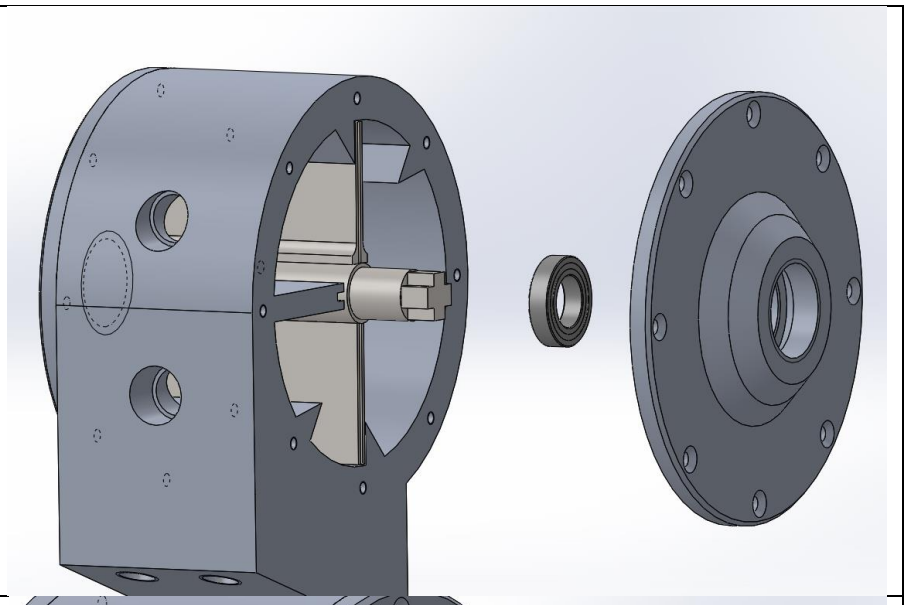
12. Add O-rings to sealing screw as described in steps 6-7 and then screw in the sealing screw	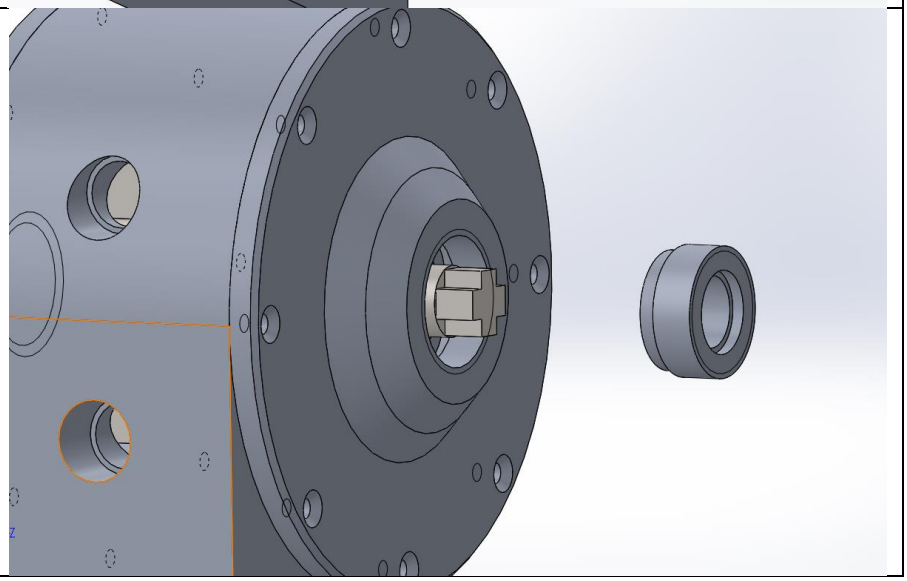

13. Add load bearing sides to both sides of axle	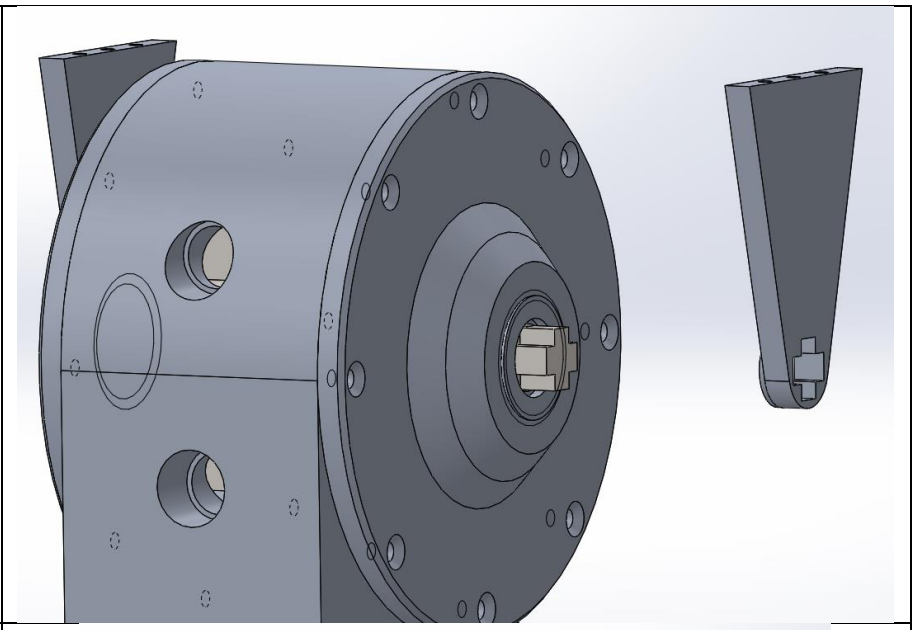
14. Add pyramid on top of load bearing sides and fix using M2 screws	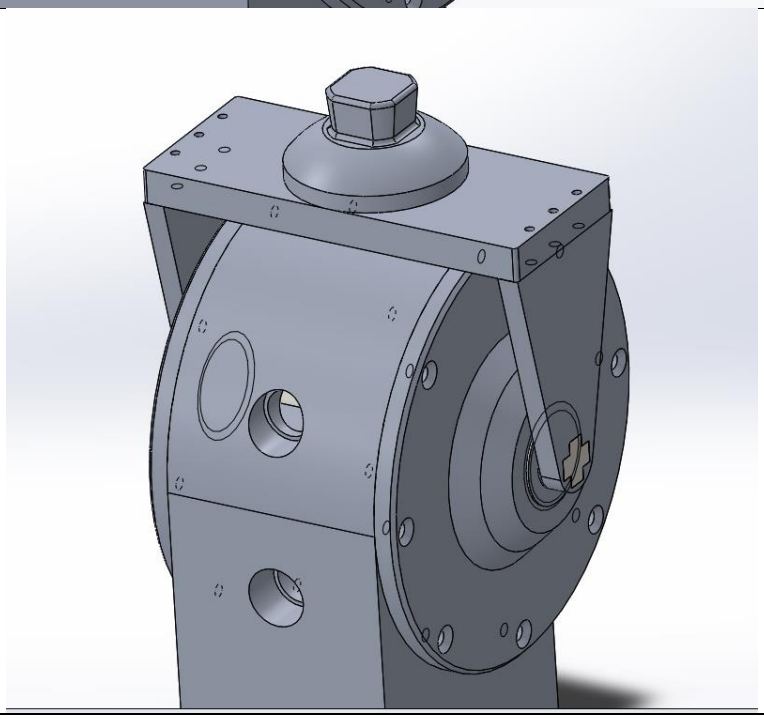

15. Using M10 screws, fix main housing to carbon fiber foot	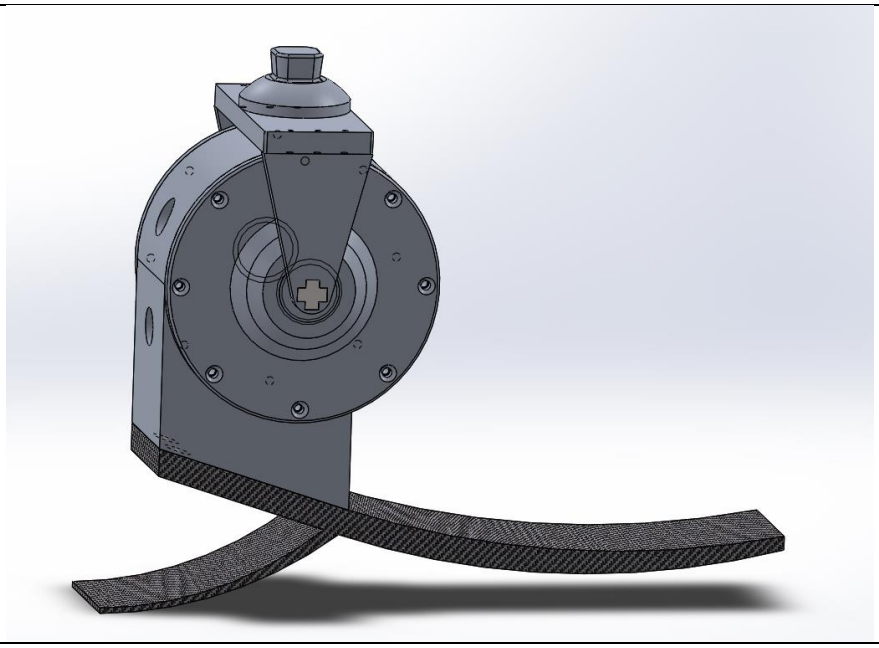

Appendix B – 2D Work Drawings

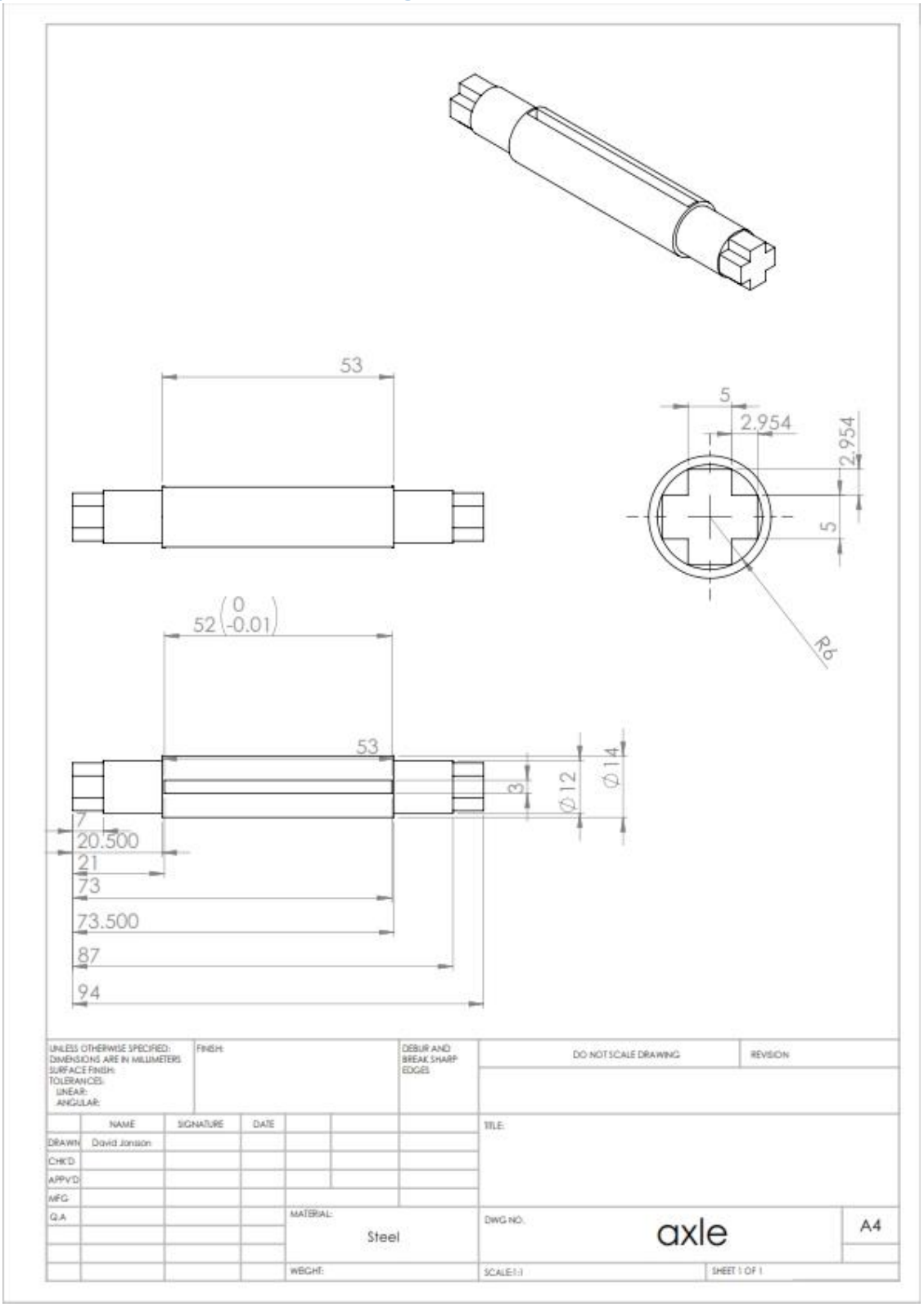

Figure B. 1: Axle Work Drawing

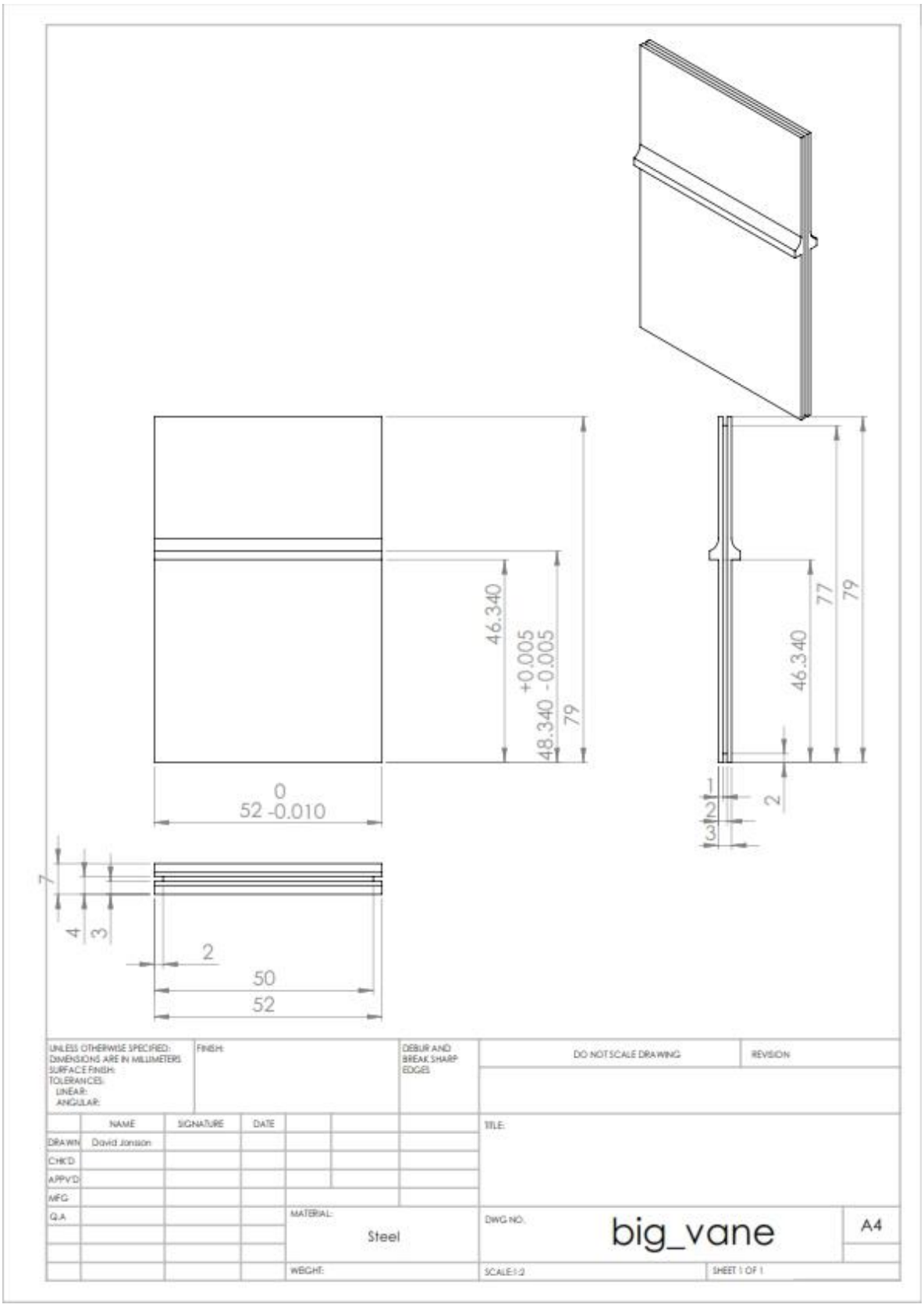

Figure B. 2: Vane Work Drawing

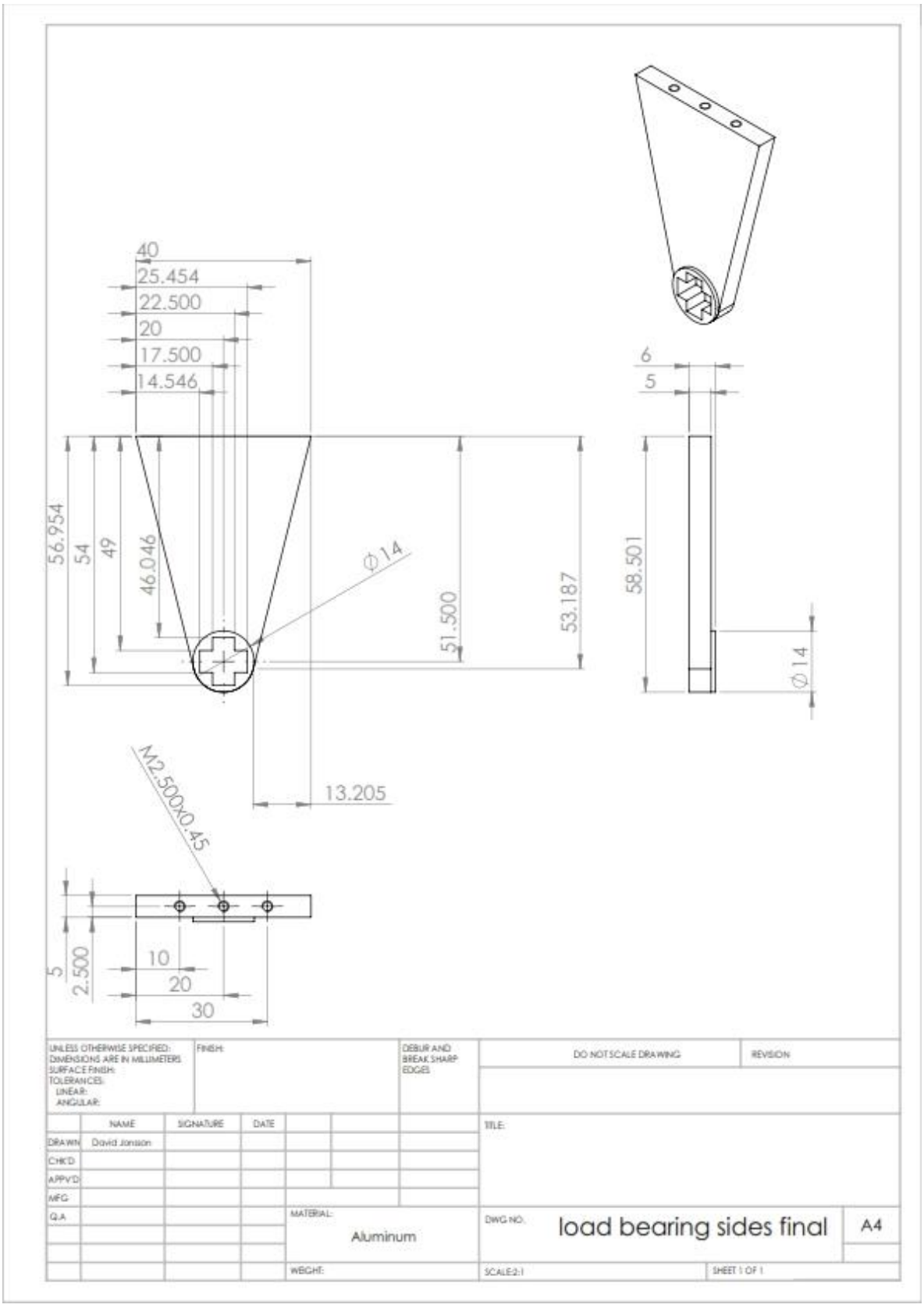

Figure B. 3: Load Bearing Sides Work Drawing

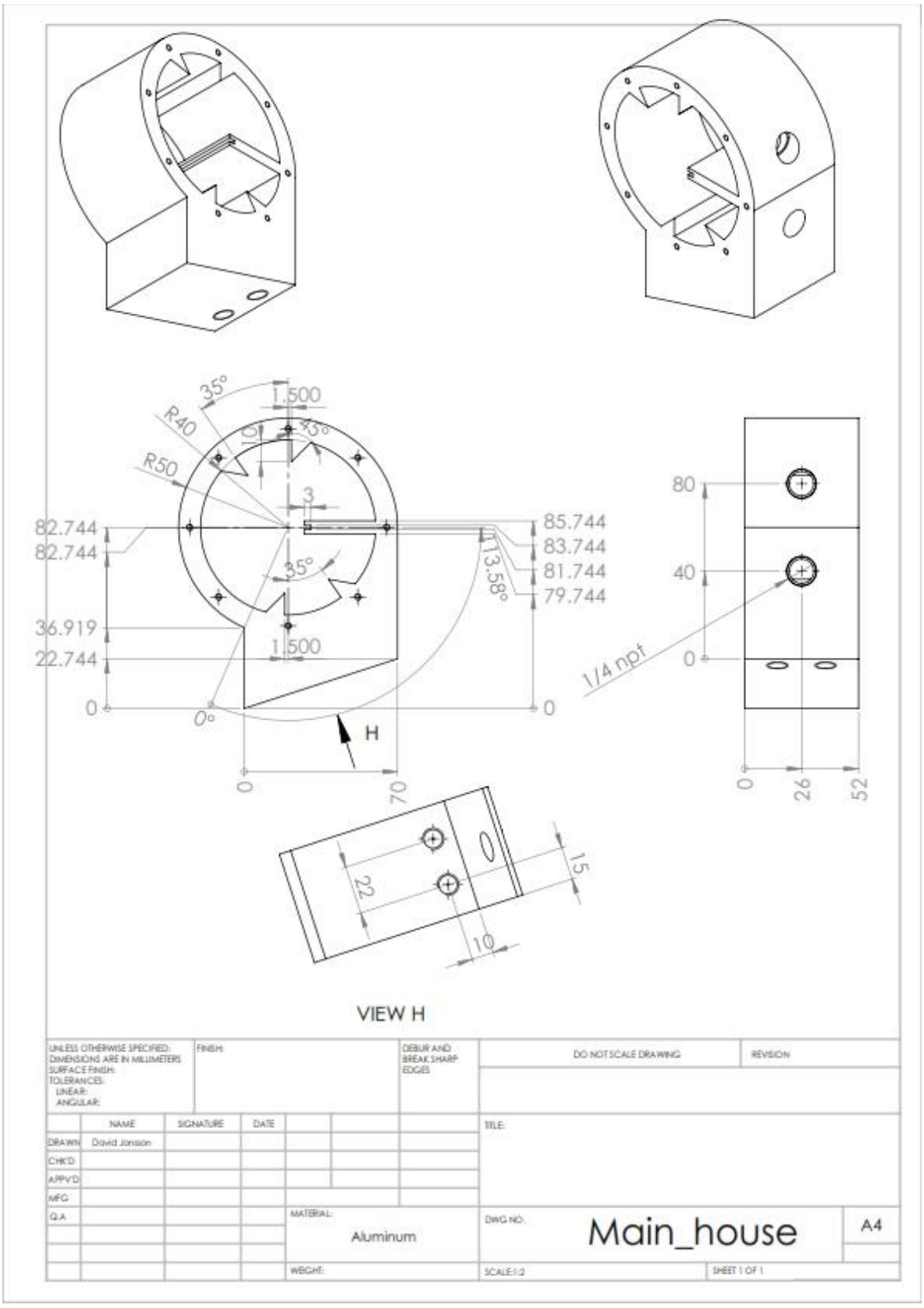

Figure B. 4: Main Housing Work Drawing

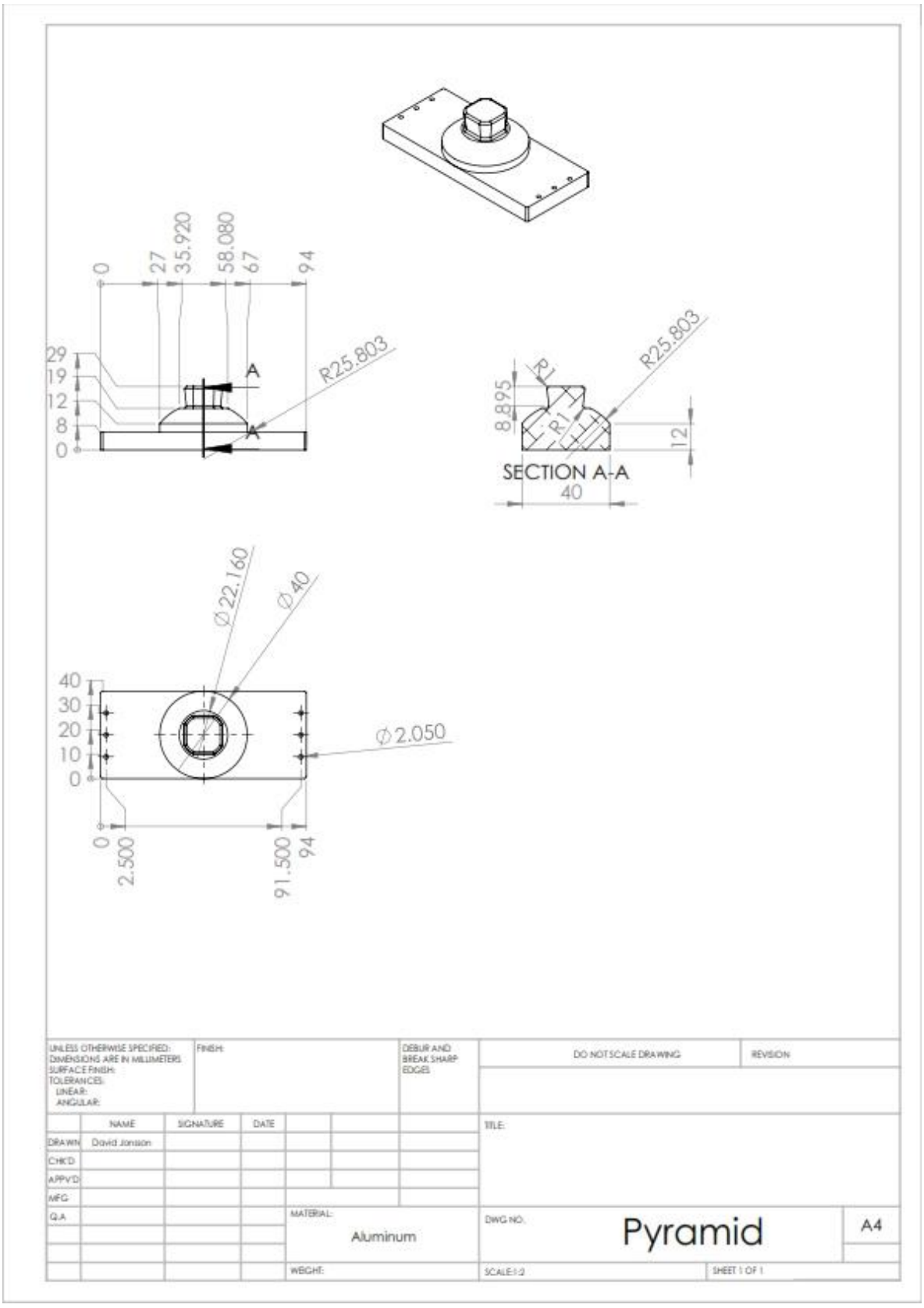

Figure B. 5: Pyramid Work Drawing

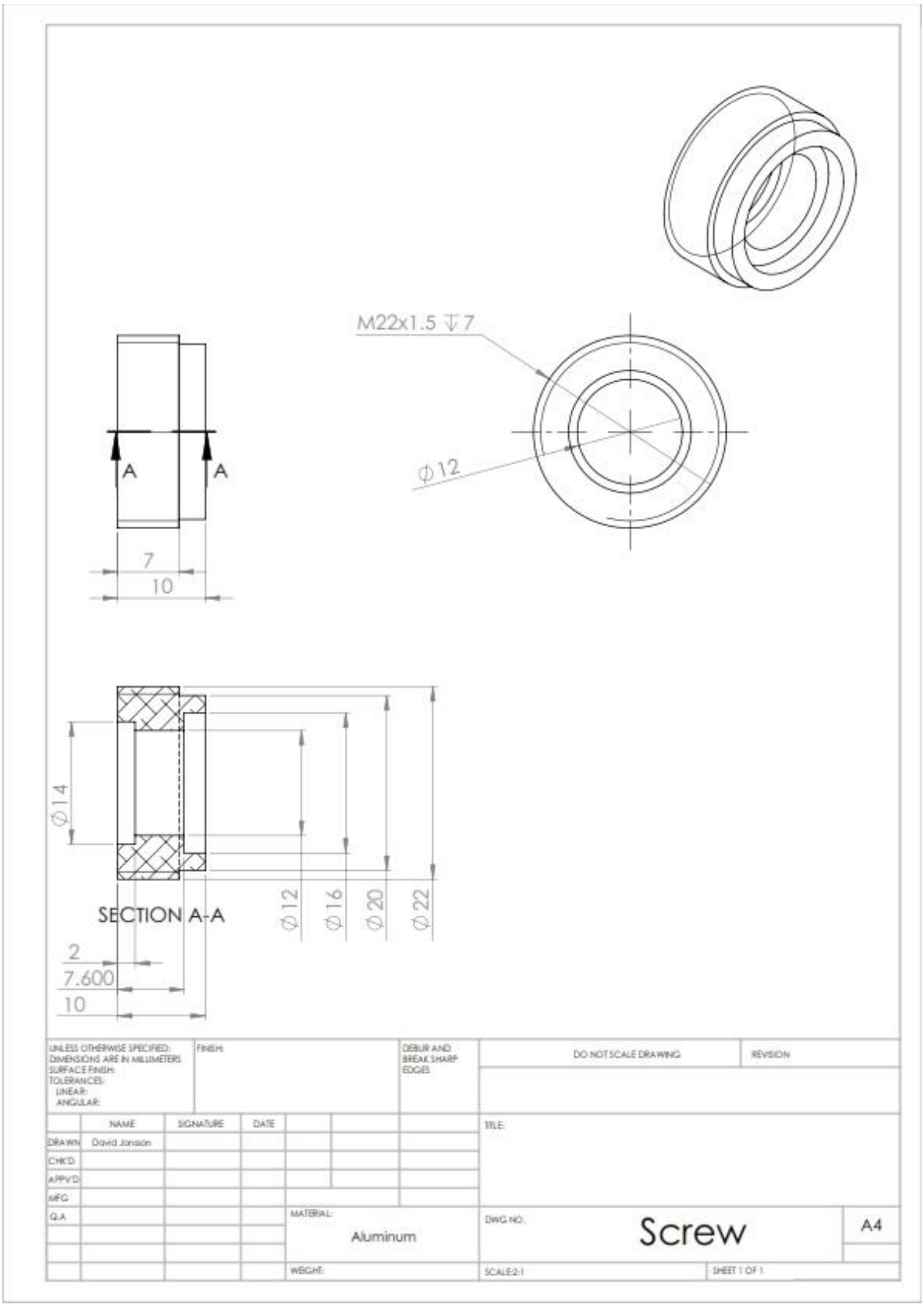

Figure B. 6: Screw Work Drawing

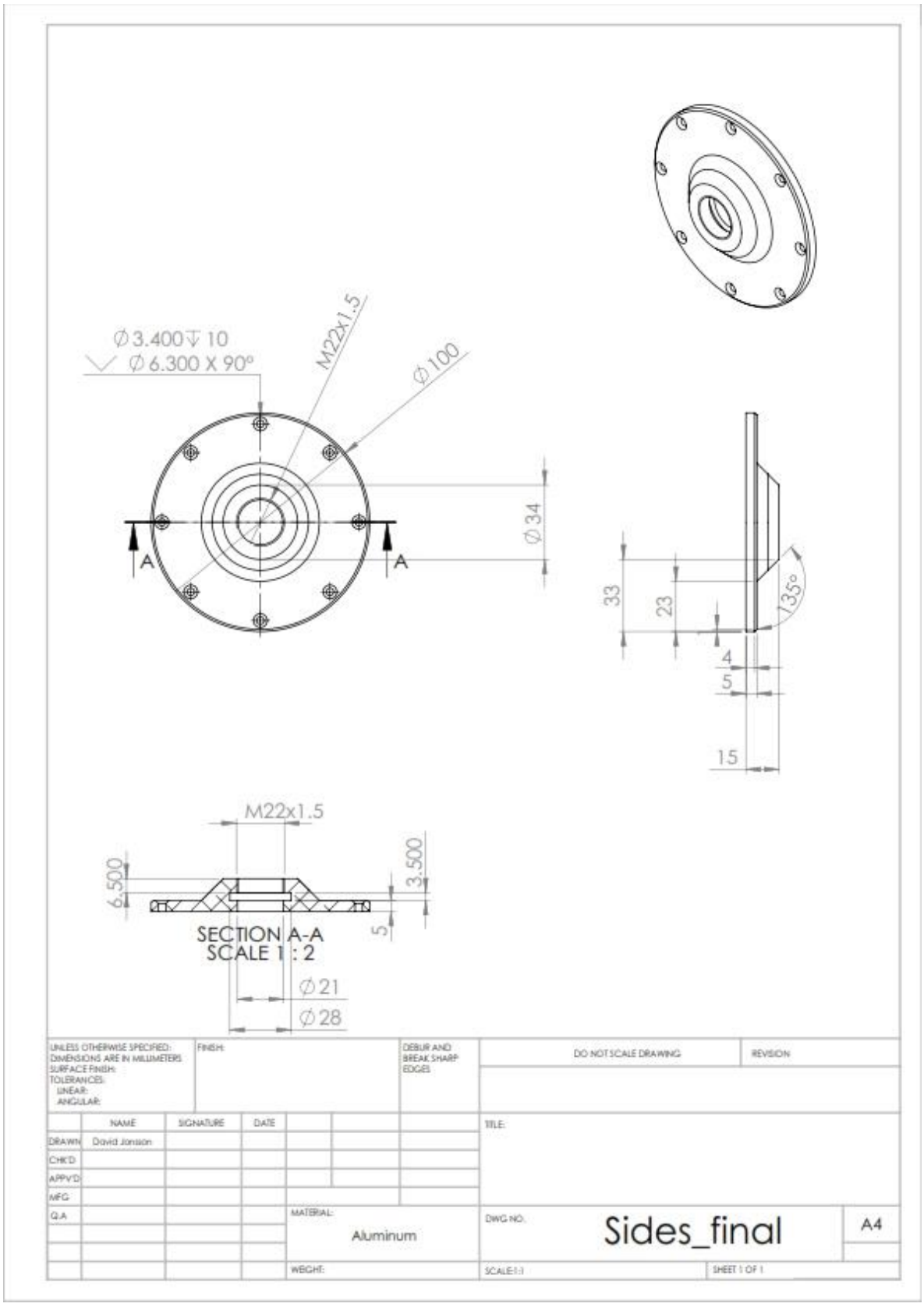

Figure B. 7: Sides Work Drawing

Appendix C – Bill of Materials (BOM)

Component name	#Required
Axle	1
Vane	1
Load Bearing Sides	2
Main House	1
Pyramid	1
Screw	2
Sides	2

Table C. 1: BOM for machined components

Component name	#Required	McMaster-Carr Item nr.
High-Strength Multipurpose Neoprene Rubber	1	85785K22
Submersible Stainless Steel Solenoid Valve	1	5077T144
Multipurpose O-Ring, 19mm,3mm	1	9262K428
Metric Steel Ball Bearing	2	5972K276
Multipurpose O-Ring,19mm,3.5mm	1	9262K792
Multipurpose O-Ring,10.3mm, 2.4mm	1	9262K222
Lightweight Hydraulic Hose, 1/4 NPT Male Fittings, 1/2" OD, 2750 PSI, 1' Long	1	5201K73

Table C. 2: BOM for off the shelf components from McMaster-Carr